Reaction of Acid-Activated Mitomycin C with Calf Thymus DNA and Model Guanines: Elucidation of the Base-Catalyzed Degradation of *N*7-Alkylguanine Nucleosides†

Maria Tomasz,*,‡ Roselyn Lipman,‡ Min S. Lee,§ Gregory L. Verdine,§ and Koji Nakanishi*,§

Department of Chemistry, Hunter College, The City University of New York, New York, New York 10021, and Department of Chemistry, Columbia University, New York, New York 10027

Received September 16, 1986; Revised Manuscript Received November 19, 1986

ABSTRACT: Mitomycin C (MC, **1**) forms covalent adducts under acidic activating conditions (pH ~4) with deoxyguanosine, d(GpC), and guanine residues of calf thymus DNA. In the case of deoxyguanosine, five adducts arise from a common precursor, *N*7-(2″β,7″-diaminomitosen-1″-yl)-2′-deoxyguanosine (**10a**; not isolated), which hydrolyzes spontaneously via two pathways: (i) scission of the glycosidic bond to form *N*7-(2″β,7″-diaminomitosen-1″α-yl)guanine (**5**) and its 1″β-isomer (**6**) and (ii) imidazolium ring opening to generate three 2,6-diamino-4-hydroxy-5-(*N*-formyl-2″β,7″-diaminomitosen-1″β-yl)pyrimidine (FAPyr) derivatives that are substituted at N^6 by isomeric 2′-deoxyribose units [i.e., 1′β-furanose (**7**), 1′α-furanose (**8**), and 1′β-pyranose (**9**)]. The structures of **5**–**9** were determined by spectroscopic methods. The same five adducts were obtained from d(GpC), but only the guanine adducts **5** and **6** were formed in DNA. Adducts **7**–**9** interconvert during high-performance liquid chromatography (HPLC). The unexpected isomerization of the deoxyribose moiety of the initially formed 1′β-furanose adduct **7** to those of **8** and **9** occurs upon imidazolium ring opening, as discerned by the course of imidazolium cleavage of the simple models *N*7-ethyl- and *N*7-methylguanosine and *N*7-methyl-2′-deoxyguanosine. All ring-opened *N*7-alkylguanosine derivatives studied here exist as a mixture of distinct *N*-formyl rotamers, manifested by multiple interconverting peaks on HPLC and in the ^1H NMR spectra. In the UV spectra of such derivatives, a new and diagnostic maximum at 218 nm (at pH 7) is observed. Acid-activated MC is found to alkylate preferentially the Gua-N7 position in deoxyguanosine or d(GpC), in contrast to reductively activated MC, which preferentially alkylates the Gua-N^2 position. This finding is explained by the different electronic structures of acid- and reduction-activated MC. In DNA, the N7 specificity of acid-activated MC is partially offset by steric factors.

Mitomycin C (MC;[1,2] **1**), the potent antibiotic and clinically useful antitumor agent, binds covalently to DNA in vitro and in vivo (Szybalski & Iyer, 1967). At physiological pH, the latent DNA-alkylating function of MC must be unmasked by enzymatic or chemical reduction; thus, MC represents a prototypical example of the class of substances that functions as "bioreductive alkylating agents" (Lin et al., 1976; Moore, 1977). Reduction of the MC quinone function triggers a sequence of reactions in which (i) methanol is expelled from the 9/9a positions and (ii) the 1,2-aziridine moiety is opened with stereorandom capture of nucleophiles at exclusively the 1-position (Iyer & Szybalski, 1964; Tomasz & Lipman, 1981; Hornemann et al., 1983; Bean & Kohn, 1983). The MC derivatives thus obtained are generally reoxidized upon isolation (Tomasz & Lipman, 1981) to yield 1-substituted 2β,7-diamino "mitosenes",[3] **2**, in which Y represents the nucleophilic species captured upon aziridine cleavage. Products of reductively activated MC (MC^{*H}) with DNA constituents have recently been characterized. The major adduct formed in the reaction of MC with the dinucleoside phosphate d(GpC) was shown to be **3**, where the attacking nucleophilic group is the 2-amino function of Gua and the 1,2-stereochemistry is trans; the minor 1,2-cis isomer **4** was also obtained and characterized (Tomasz et al., 1983,[4] 1984, 1986a). The corresponding reaction of MC with calf thymus DNA (ctDNA) or poly(dG-dC)·poly(dG-dC) is highly specific, with adduct **3** accounting for over 90% of the total adduct pool; the remainder of DNA-bound MC was present in the form of the

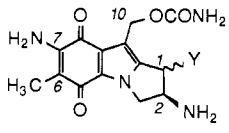

2
2a: Y = α-OH
2b: Y = β-OH

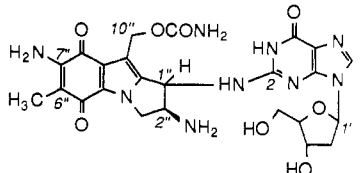

trans M-dG_{II}, **3**: 1″α-
cis M-dG_{II}, **4**: 1″β-

† This work was supported by NIH Grants GM 34509 (to K.N.) and CA 28681 (to M.T.) and PSC-CUNY Faculty Research Award 14 (to M.T.).

‡ The City University of New York.
§ Columbia University.

[1] Abbreviations: MC, mitomycin C; M, 2β,7-diaminomitosen-1-yl (cf. footnote 3); ctDNA, calf thymus DNA; P_i, inorganic phosphate; SVD, snake venom diesterase; UMP, uridine 5′-monophosphate; Gua, guanine; MC^{*H}, reductively activated mitomycin C; MC^{*+}, acid-activated mitomycin C; (FT)IR, (Fourier transform) infrared; SEDIR, second-derivative infrared; SEDUV, second-derivative ultraviolet; HPLC, high-performance liquid chromatography; FAPyr, formamidopyrimidine (cf. structure I); *N*7-HEG, *N*7-(2-hydroxyethyl)guanine; Tris, tris(hydroxymethyl)aminomethane; NOE, nuclear Overhauser effect; ppm, parts per million; br, broad; s, singlet, d, doublet; dd, doublet of doublets; m, multiplet; exch, exchangeable.

[2] Recent X-ray studies have shown that the absolute configuration of MC should be depicted as in structure **1** and not as that generally accepted prior to 1983 (Shirahata & Hirayama, 1984). Independent CD results are in accord with the findings of Shirahata and Hirayama (Verdine & Nakanishi, 1985b).

[3] The term "mitosene" refers to the structure as in **2**, without substituents at the 1-, 2-, and 7-positions (Webb et al., 1962).

[4] These compounds were originally stated to be linked via Gua-O^6 to the mitosene C-1″ (Tomasz et al., 1983, 1984). A reinvestigation of this structural assignment revealed that the correct structures are **3** and **4** (Tomasz et al., 1986a).

0006-2960/87/0426-2010$01.50/0

minor adducts **4**, 10″-decarbamoyl-**3**, and a newly discovered bis adduct (see below; Tomasz et al., 1986b). The latter results are in contrast with previous reports indicating that nuclease P_1 digestion of MC-modified DNA yields three MC–mononucleotide adducts, in which the mitosene moiety is linked to the N^2- and O^6-positions of guanine and the N^6-position of adenine (Hashimoto et al., 1982, 1983, 1984). The latter results could not be reproduced or substantiated in our laboratory (Tomasz et al., 1986b), and this aspect is currently under further investigation. As mentioned above, a bis adduct formed between MC and two deoxyguanosine residues was isolated from MC-modified DNA, and its molecular structure has been elucidated. This new adduct is formed in reactions of reductively activated MC with poly(dG-dC)·poly(dG-dC) or genomic DNA in vitro (Tomasz et al., 1987); its bis substitution indicates that it is the long-sought "cross-link" produced in DNA upon treatment with reductively activated MC (Szybalski & Iyer, 1967).

It has been observed that MC also can be activated in the absence of reducing agents by simply lowering the pH of the reaction medium to a value of ≤5 ("acidic activation"). Under these conditions, both monofunctional binding and cross-linking of MC to DNA occurs (Lown et al., 1976; Lown & Weir, 1978). A chemical study utilizing model nucleophiles (e.g., P_i, UMP) demonstrated that acidic activation is sufficient to trigger aziridine opening and nucleophilic capture to yield mitosenes **2**; thus, both reductive and acidic conditions give rise to derivatives possessing a 1-substituted 2β,7-diaminomitosene moiety (Tomasz & Lipman, 1979). In view of this apparent similarity of chemical reactivity of MC under completely different activation conditions, we undertook a study of the reaction of acid-activated MC (MC^{*+}) with DNA and DNA constituents. [A brief account of some of the work reported in this paper has been published (Tomasz et al., 1985)].

In order to facilitate a direct comparison of acidic with reductive activation, we first chose the model DNA substrate d(GpC) since this dinucleoside phosphate was previously shown (Tomasz et al., 1983,[4] 1986a) to yield **3** as the major adduct when reacted with reductively activated MC. We report here that (i) under acidic conditions MC–d(GpC) adducts are readily formed but (ii) they are different from those formed in the reaction of MC^{*H} with d(GpC), i.e., **3** and **4**. Thus, under the present acidic conditions we have obtained and characterized, in addition to the previously known N^2 adducts **3** and **4** (minor adducts), a new set of MC adducts (**5–9**) that arise from linkage of the mitosene moiety to the N7-position of Gua, indicating a remarkable switch from N^2 (reductive) to N7 (acidic) as the preferentially alkylated position on Gua, depending on the activation medium of MC. A similar result was obtained in the acidic reaction of MC with DNA; the major products thus obtained are **5** and **6**, in addition to the previously characterized N^2 adduct **3**.

Alkylation of genomic deoxyguanosine residues at the N7-position is known to occur as a result of exposure to a wide variety of natural and synthetic carcinogens, mutagens, and antitumor agents including aflatoxin B_1, nitrogen mustards, and alkylnitroso compounds (Singer & Grunberger, 1983; Croy et al., 1978). The initially formed *N*7-alkyl-Gua residues are hydrolytically labile and rapidly decompose via two discreet pathways: (i) scission of the glycosidic linkage to form the corresponding *N*7-alkylguanine and (ii) imidazolium ring opening to generate an *N*7-alkylformamidopyrimidine (N7-alkyl-FAPyr) nucleoside (vide infra; Lawley & Brookes, 1963). See structure I for our numbering system. Though numerous

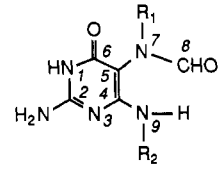

I

studies have appeared in the literature concerning the chemical structure of *N*7-alkyl-FAPyr residues, their exact nature has previously eluded complete description. We demonstrate here that the initially formed *N*7-mitosenyl adduct **10** decomposes via both available hydrolytic pathways to yield (i) the isomeric pair of *N*7-mitosenylguanines **5**/**6** and (ii) a series of imidazolium ring opened *N*7-mitosenyl-FAPyr deoxyribosides possessing rearranged sugar moities (**7–9**; Scheme I). The latter set of compounds displayed room temperature interconversion on HPLC and identical difference UV spectra that were characteristic of *N*7-alkyl-FAPyr ribosides. Elucidation of the precise nature of these imidazolium-cleaved mitosene adducts was facilitated by a parallel investigation of the basic hydrolysis of the model compound *N*7-ethylguanosine (**11**). In contrast to previous reports that have suggested that **11** hydrolyzes to a single homogeneous substance, i.e. **13**, we have now determined that imidazolium ring cleavage of **11** proceeds rapidly by rearrangement of the β-ribofuranoside function (via imine **12**) to yield three *N*7-ethyl-FAPyr compounds, **13–15**, which equilibrate in solution (see below). The structures of **13–15** were arrived at by chemical derivatization to the corresponding triacetates **16–18** followed by spectroscopic measurements. Examination of the basic hydrolysis of *N*7-methylguanosine (**26**) reveals that it degrades by the same course as **11** to give the isomeric *N*7-methyl-FAPyr ribosides **27–29**, though different reaction kinetics are observed in the two cases. Additionally, we have determined that the deoxyribose analogue *N*7-methyl-2′-deoxyguanosine (**19**), which possesses the same β-D-2′-deoxyribose sugar moiety as the mitosene adduct intermediate **10**, also rearranges upon basic hydrolysis to give three major *N*7-methyl-FAPyr compounds (**20–22**).

In light of these results, we postulate that the rearrangement of the sugar portion of *N*7-alkyl-FAPyr ribosides and 2′-deoxyribosides (Scheme II) is a general phenomenon. Furthermore, the inherent complexity of the mixtures generated from basic hydrolysis of *N*7-alkylguanosines appears to result from two factors: (i) facile interconversion of the isomeric furanose and pyranose ribosides and (ii) the existence of discreet, interconverting *N*-formyl rotamers. The potential significance of these findings with regard to N7-alkylation of Gua residues by MC and other DNA alkylators in vivo will be discussed herein.

Experimental Procedures

Materials

Most materials used in this work have previously been described [Tomasz et al., 1983, 1985, 1986b; Verdine and Nakanishi (1985a) and references cited therein]. Additional materials and their sources are as follows: *N*7-methylguanosine, Sigma Chemical Co., St. Louis, MO; *N*7-methyl-2′-deoxyguanosine prepared as described in Farmer et al. (1973); *N*7-(2-hydroxyethyl)guanine synthesized as described in Brookes and Lawley (1961).

Methods

Reaction of **1** *with d(GpC) under Acidic Activation Conditions.* A solution of d(GpC) (18 μmol) in 1.0 mL of water

Scheme I: Products Resulting from the Acid-Catalyzed Reaction of MC (**1**) with d(GpC)[a]

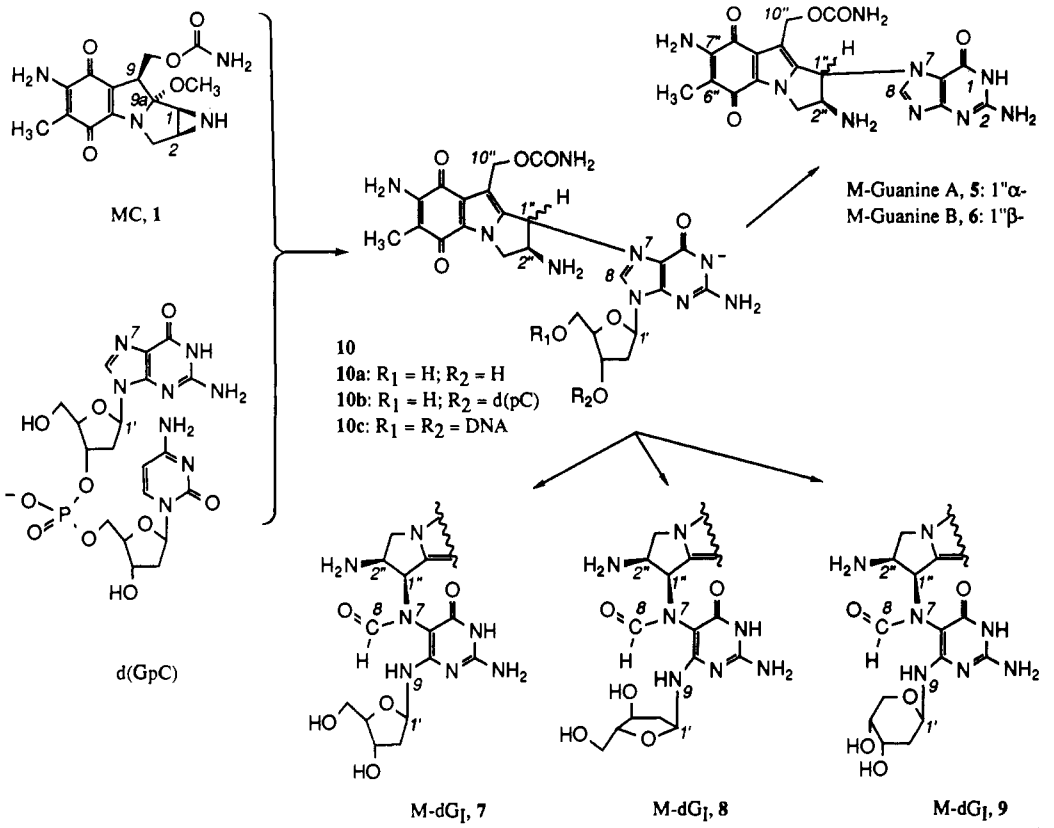

[a] Intermediate **10** has not been isolated. M in **5–9** denotes the mitosene moiety. Products **7–9** are collectively termed M–dG_I.

Scheme II: Products Resulting from Mild Base Treatment of *N*-Ethylguanosine (**11**) and Homologues **19** and **26**[a]

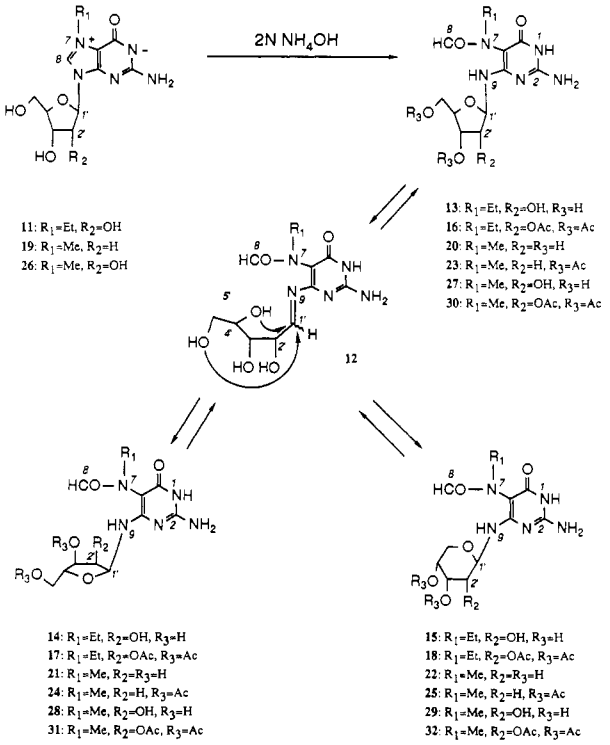

[a] Imine **12** has not been isolated.

was acidified to pH 3.5–4.0 by addition of appropriate amounts of cation-exchange resin (Bio-Rad, AG 50W-X-B, H^+ form, 20–50 mesh). The beads were removed by filtration, and MC (20 μmol) was added (dissolved in 1.0 mL of H_2O). The total volume of the aqueous solution was adjusted to 2.5 mL and maintained at pH 3.5–4.0 by periodic additions of 0.01 N HCl. After 3.5 h, 25 °C, the solution was neutralized with dilute NaOH and chromatographed on Sephadex G-25 (see below).

Enzymatic digestion of the adduct fraction M–d(GpC) was carried out by the action of snake venom diesterase (SVD) as previously described (Tomasz et al., 1983).

Reaction of MC with deoxyguanosine was carried out as above, substituting deoxyguanosine for d(GpC) in the reaction protocol.

Reaction of MC with DNA under Acidic Activation. Calf thymus DNA (20 μmol) and MC (20 μmol) were dissolved in 3 mL of 0.015 M Tris buffer (pH 7.2), and the solution was adjusted to pH 4 by addition of dilute HCl. The reaction was gently stirred for 4 h, 25 °C, during which time the pH was maintained at a value of 3.5–4.5 by periodic additions of dilute HCl. The mixture was then neutralized with 0.5 M NH_4HCO_3 and placed directly onto a 5 × 56 cm Sephadex G-100 column and eluted with 0.02 M NH_4HCO_3.

The MC–DNA complex (void volume fraction from above Sephadex G-100 column) was lyophilized and redissolved in 0.01 M Tris (pH 6.8; supplemented with 0.001 M $MgCl_2$) to a concentration of 3 OD_{260} units/mL. Enzymatic digestion was carried out at 37 °C by successive addition of the following: (1) DNase I (16 units/OD_{260} unit) at 0 h; (2) after adjustment to pH 8.5, SVD (1.25 units/OD_{260} unit), two additions at 2 and 4 h; (3) alkaline phosphatase (0.5 unit/OD_{260} unit), at 6 h, with incubation continued until 24 h. The resulting mixture was filtered through a Whatman No. 1 paper disc in vacuo and analyzed directly by HPLC (see below).

Separation of Products. (a) Sephadex G-25 (fine) column chromatography using 0.02 M NH_4HCO_3 as eluant was performed as described (Tomasz & Lipman, 1979; Tomasz et al., 1983). (b) HPLC separations for all adduct reactions utilized a Beckmann Model 330 system equipped with a UV

monitor (254 nm) and an Ultrasphere-ODS column (1.0 × 25 cm; 8:92 CH_3CN/0.02 M aqueous potassium phosphate, pH 5.0; 2.0 mL/min). Fractions were desalted by rechromatography on a Sephadex G-25 column (0.02 M NH_4HCO_3 eluent); solvent and buffer were removed by lyophilization.

Quantitative analysis of all substances was accomplished by UV spectrophotometry as previously described (Tomasz & Lipman, 1979). The spectral properties of **5** and **6** were determined in the present work to be as follows: **5**, ϵ_{299} = 11 540; **6**, ϵ_{299} = 11 650 (0.01 M potassium phosphate, pH 7.0). A more detailed analysis of the UV of these compounds has been briefly reported elsewhere (Verdine & Nakanishi, 1985a).

Hydrolysis/Acetylation and Purification of Model N7-Alkylguanosines. Model *N*7-alkylguanosines **11**, **19**, and **26** were hydrolyzed in 2 N NH_4OH at a concentration of 8.0 mg/mL, 2 h, 25 °C, frozen immediately in a liquid N_2 bath, and lyophilized overnight to yield white powders. Acetylations were carried out by dissolving the powdered hydrolysis mixtures in dry pyridine to a concentration of 0.1 mM, 25 °C, followed by addition of 1 mg of 4-(*N*,*N*-dimethylamino)-pyridine and 2 mol equiv (for each hydroxyl group present) of freshly distilled acetic anhydride. The reaction was allowed to proceed for 30 min, and the solvent was then removed in vacuo. Longer reaction times led to some acetylation of the FAPyr 2-NH_2 function. The crude reaction mixtures were redissolved in 10:90 MeOH/$CHCl_3$, applied to preparative silica gel TLC plates (Analtech preadsorbent, 20 × 20 cm, 500 μm), and eluted sequentially with 10:90 and then 20:80 CH_3OH/$CHCl_3$ (20 mg of hydrolyzed starting material per plate). The R_f of **16** is 0.59 while **17** and **18** coelute at R_f 0.69. Additional purification, when necessary, was carried out on HPLC with an IBM-ODS column (1.0 × 25 cm), a 15:85 CH_3CN/H_2O as eluent, a 3.0 mL/min flow rate, and 254-nm detection; peaks were collected into flasks maintained in a −78 °C bath; **16** and **17** coelute at a retention time of 39 min, and **18** elutes at 27 min.

Kinetic Study of the Hydrolysis of N7-Ethylguanosine (**11**). A total of 340 mg of **11** was dissolved in 42.5 mL of 2 N NH_4OH in a round-bottom flask with vigorous stirring to effect immediate dissolution. Samples of 1.25 mL were withdrawn at appropriate time intervals, frozen immediately, and lyophilized overnight. Each lyophilized sample was redissolved in 600 μL of 80:20 Me_2SO-d_6/MeOH-d_4 and the ^1H NMR spectrum recorded immediately. Careful integration of the anomeric peak signals (5–6 ppm region) was used to quantitate the amounts of **13**–**15** present in each sample. The isomer ratios of individual NMR samples did not change over a period of >1 week at room temperature.

Perchloric Acid Hydrolysis of Adducts. The pure adduct (0.05 μmol) was incubated with 50 μL of 70% aqueous $HClO_4$ in a sealed test tube at 100 °C for 1 h, then diluted with water, and neutralized with KOH solution. The resulting $KClO_4$ precipitate was removed by filtration and the supernatant analyzed by HPLC with 0.03 M potassium phosphate (pH 6.0) for elution. Standard elution times were as follows: cytosine, 10 min; guanine, 22 min.

Spectroscopic Techniques

^1H NMR spectra were recorded on either a Bruker WM-250 or a Jeol GX-400 (250 and 400 MHz, respectively); Me_2SO-d_6 was the solvent, except where otherwise indicated. Deuterium-exchange experiments employed MeOH-d_4. Chemical shifts are reported in parts per million (ppm) downfield from external tetramethylsilane.

Solution FTIR spectra were recorded in Me_2SO-d_6 on an IBM IR85 instrument, MCT detector, 2-cm^{-1} resolution, using an ATR CIRCLE microcell (Barnes Analytical). Details of the data-handling protocol have been reported in detail elsewhere (Verdine & Nakanishi, 1985; Tomasz et al., 1986a).

CD spectra were obtained on either a Jasco J40 or a J500A spectropolarimeter in MeOH solution and were base line corrected.

UV spectra were recorded on either a Perkin-Elmer Model 320 spectrophotometer/Model 22 computer or a Cary Model 213; solvents are as indicated in text.

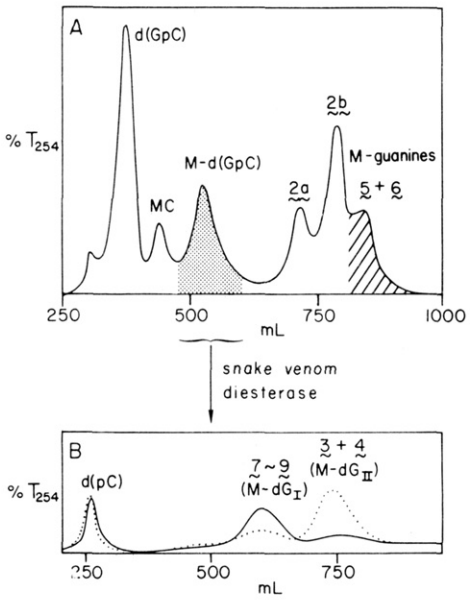

FIGURE 1: (A) Sephadex G-25 elution profile of the crude reaction mixture resulting from treatment of **1** with d(GpC) under mild acid catalysis: stippled peak, M–d(GpC) adduct fraction; hatched peak, M–guanines fraction. (B) Sephadex G-25 elution profile of the products arising from treatment of the M–d(GpC) adduct fraction in (A) with snake venom diesterase. Solid line, products obtained under current acidic activation conditions; dotted line, products obtained under reductive activation of MC (Tomasz et al., 1983).

RESULTS

Reaction of MC with d(GpC) under Acidic Activation Conditions. Shown in Figure 1A is the Sephadex G-25 elution profile of the reaction mixture resulting from treatment of MC^{*+} with d(GpC) (Methods). The bands were assigned on the basis of comparison with the previously reported products arising from treatment of d(GpC) with MC^{*H} (Tomasz et al., 1983). Thus, unreacted starting materials [d(GpC) and MC] eluted first, followed by the M–d(GpC) adduct fraction (stippled peak) and the isomeric MC solvolysis products **2a** and **2b**. The last band (hatched peak), designated "M-guanines" (**5** and **6**), was not previously observed in any reaction mixtures resulting from reductive activation of MC.

The M–d(GpC) fraction (Figure 1A, stippled peak) was hydrolyzed by treatment with SVD and subjected to Sephadex G-25 chromatography. As seen in Figure 1B (solid line), SVD treatment of the M–d(GpC) fraction leads to the release of 2′-deoxycytidine 5′-phosphate, d(pC), and two MC–deoxyguanosine adduct fractions, designated M–dG_I and M–dG_{II} (ratio >90:10). Interestingly, SVD hydrolysis of the analogous M–d(GpC) fraction obtained from reductive activation of MC (shown in Figure 1B, dotted line, for purposes of comparison) was previously shown (Tomasz et al., 1983) to yield the same two adduct fractions as those obtained presently; however, in the latter case, the ratios of the two fractions were reversed from that seen in this work (M–dG_I:M–dG_{II} = ca. 15:85; Figure 1B, dotted line). M–dG_{II} has previously been shown

Table I: Yields and Distribution of MC Adducts Formed under Various Conditions

entry	substrate	activation condition	% yield[a] 5	6	7–9	3	relative distribution 5	6	7–9	adduct % ratio, N7/(N7 + N2)
A[b]	d(GpC)	reductive	0.00	0.00	0.84	6.0	0.0	0.0	1.0	12.3
B	d(GpC)	acidic	1.7	0.1	2.1	0.2	1.0	0.05	0.08	95.1
C	GpC	acidic	0.0	0.0	5.0[c]	0.25[d]	0.0	0.0	1.0	95.2
D[b]	dG	reductive	0.0	0.0	~1	9.5[e]	0.0	0.0	~1.0	~9.5
E	dG	acidic	7.8	2.6	7.0	1.2[e]	1.0	0.3	0.9	93.5
F	dG	acidic[f]	5.0	2.2	7.7	nd	1.0	0.4	1.5	nd
G	G	acidic	0.04	0.02	3.0[c]	nd	1.0	0.5	75.0	nd
H	ctDNA	acidic	1.2	0.5	0.0	1.7	1.0	0.4	0.0	50.0
I[g]	ctDNA	reductive	0.0	0.0	0.0	10.0[e]				na

[a] Based on starting MC; determined by UV (Methods). [b] Data taken from Tomasz et al. (1983, 1986a). [c] These products are actually the ribose analogues of 7–9. Their spectroscopic and HPLC behavior are similar to those of 7–9 [d] This product is the ribose analogue of 2; its UV is identical with that of 3. [e] Combined yield of 3 and 4; ratios of 3:4 are 1.00:0.83 (entry D), nd (entry E), and 1.00:0.5 (entry I). [f] Reaction mixture not neutralized before charging onto Sephadex G-25 column; 0.02 M potassium acetate, pH 4.8, eluent used. [g] Taken from data in Tomasz et al. (1986b).

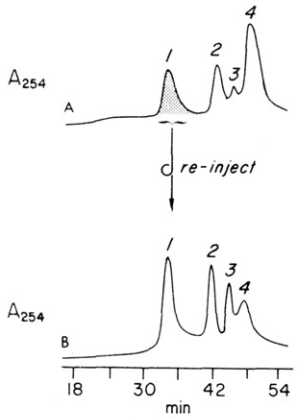

FIGURE 2: HPLC of the M–dG_I adduct fraction (mixture of 7–9). Reinjection of peak 1 (stippled peak) in (A) regenerates all four components, as shown in (B). Individual structures within the 7–9 set have not been assigned to any given HPLC peak owing to rapid equilibration of the components.

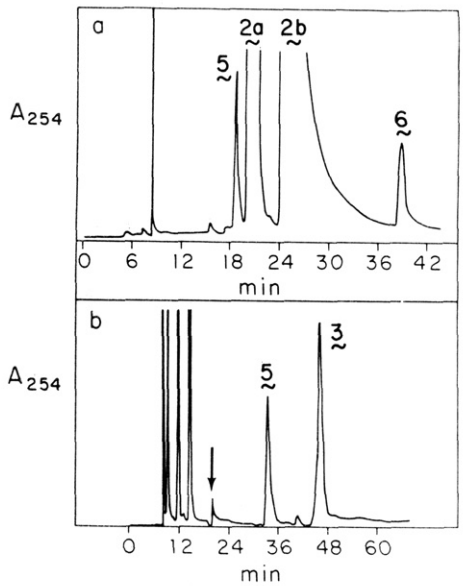

FIGURE 3: HPLC detection of adducts formed between calf thymus DNA and acid-activated MC. (a) Low molecular weight fraction (1500-mL elution volume) from Sephadex G-100 chromatography of the MC^{*+}–DNA reaction (Results). Eluent: 10:90 CH_3CN/0.03 M potassium phosphate (pH 5.0). (b) Enzymatic digest of the void-volume fraction (750-mL elution volume) from Sephadex G-100 column of the same reaction mixture as in (a). Eluent: 8:92 CH_3CN/0.03 M potassium phosphate (pH 5.0). Arrow: artifact due to change in absorbance scale from 1.28 to 0.04 AUFS.

to consist of cis and trans isomeric adducts 3 and 4 (Tomasz et al., 1983, 1984, 1986a).[4] The M–dG_I fraction was produced

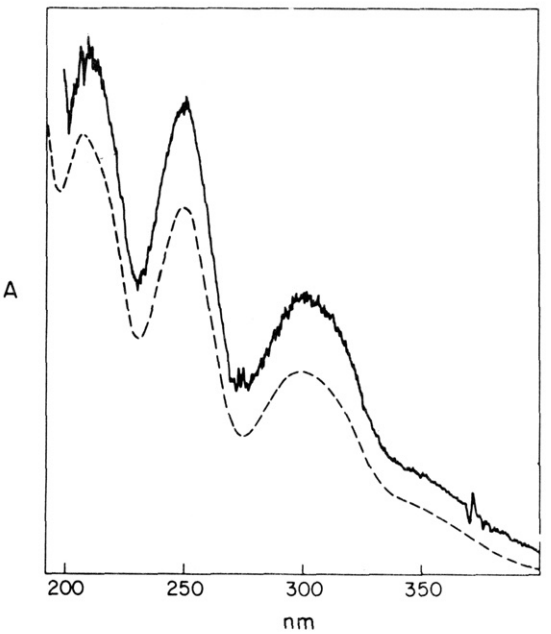

FIGURE 4: Comparison of the UV spectra of M–guanine 5 derived from dG (--), and ctDNA (—). Buffer: 0.01 M potassium phosphate, pH 7.0.

in such low yields in the previous reductive activation reactions as to preclude its characterization at that time. However, as seen in Figure 1B (solid line), it is formed in considerable amounts under the present conditions. Upon HPLC, M–dG_I consists of a series of compounds that interconvert at room temperature (Figure 2). The previously mentioned M–guanine fraction (Figure 1A, hatched peak) separates upon HPLC into two homogeneous adducts, designated M–guanine-A (5) and M–guanine-B (6) (see below).

Isolation of M–dG_I (7–9) and M–Guanines (5/6) from the Reaction of Acid-Activated MC with Deoxyguanosine. Sephadex G-25 chromatography of the crude reaction mixture (Methods) directly yielded M–dG_I (~7%) and M–guanines (~10%) (Table I, entries E and F); it is the preferred method of synthesis for preparation of M–dG_I and M–guanines.

Isolation of M–Guanines from DNA Treated with MC under Acidic Activation. The reaction mixture resulting from treatment of ctDNA with MC^{*+} (Methods) was placed directly onto a Sephadex G-100 column (5.0 × 56 cm, 0.02 M NH_4HCO_3 eluent; elution profile not shown). The MC–DNA complex eluted in the void volume (750 mL) followed by a low molecular weight MC adduct fraction (1500 mL). HPLC of the latter (Figure 3a) indicated the presence of M–guanines 5 and 6 (eluting at 20 and 39 min, respectively), as confirmed

by HPLC coinjection and UV spectral analysis with authentic samples (Tomasz et al., 1985); the simple MC solvolysis products **2a** and **2b** were also obtained. Figure 4 shows the comparison of UV spectra for **5** obtained from dG (lower trace) and DNA (upper trace); almost identical comparison spectra (not shown) were obtained for **6**. The amounts of **5** and **6** obtained correspond to respectively 0.0045 and 0.003 mol of adduct/mol of DNA base, indicating that 0.75% of the total ctDNA bases were converted into these adducts under the above conditions.

The MC–DNA complex (void volume fraction of above Sephadex G-100 column, 750 mL) was determined to have a binding ratio of 0.017 mol of MC/mol of DNA base by the spectrophotometric method previously described (Tomasz et al., 1974). This complex was digested (Methods) and analyzed directly by HPLC, the elution profile for which is shown in Figure 3b. The four early-eluting peaks in Figure 3b (~8–16 min) are the four unmodified nucleosides, followed by two peaks at 34 and 46 min. The 34-min peak was unambiguously identified as M–guanine **5** by HPLC coinjection and comparison of the Sephadex G-25 elution profiles and UV spectra with authentic **5** (as in Figure 4). The peak eluting at 46 min was identified as N^2 adduct **3** by similar comparison with an authentic sample (Tomasz et al., 1986a). The relative amounts of **5** and **3** were 0.4:1.0, indicating that 0.5 and 1.2% of all DNA bases in this stable MC–DNA complex were modified to yield **5** and **3**, respectively. Combining this yield of adducts with that spontaneously released from the DNA (above; Figure 3a), it is calculated that 0.95% of the total DNA bases are modified to yield **5** while 0.3% are modified to yield **6**. Thus, 1.25% of all DNA bases in ctDNA were modified at the Gua-N7 position (**5** + **6**) under the current acidic activation conditions. The amount of modification at Gua-N^2 (**3**) corresponds to 1.2% of the total bases. These results are further summarized in Table I, entry H.

Structure Determination of the M–Guanines. Multiple batch separations of the M–guanines on Sephadex G-25 and HPLC were performed as described above, followed by desalting and lyophilization. Thus, 2.8 and 2.3 mg of maroon **5** and **6** were obtained and shown to be homogeneous on HPLC. The following structural studies led to the assignment of structures **5** and **6** for M–guanines-A and -B.

^1H NMR Spectroscopy. [For full reproductions of the ^1H NMR spectra of **5–9** and **13–18**, see supplementary material of Tomasz et al. (1985).] The ^1H NMR spectra of **5** and **6** with Me_2SO-d_6 solvent were as follows: (**5**) δ 10.58 (exch s, 1 H, N1-H), 7.91 (s, 1 H, 8-H), 6.74, 6.58, and 6.20 [exch br s, 2 H each, 2-NH_2, 7″-NH_2, and 10a″-NH_2 (individual resonances not assigned)], 5.59 (d, 1 H, 1″-H), 4.85 and 4.22 (dd, 1 H each, 10″-H_2), 4.56 (dd, 1 H, 3″-H_b), 4.23 (br m, 1 H, 2″-H), 3.84 (dd, 1 H, 3″-H_a), 1.76 (s, 3 H, 6″-CH_3); (**6**) δ 10.96 (exch br s, 1 H, N1-H), 7.40 (s, 1 H, 8-H), 6.59, 6.38, and 6.22 [exch br s, 2 H each, 2-NH_2, 7″-NH_2, and 10a″-NH_2 (individual resonances not assigned)], 6.37 (d, 1 H, 1″-H), 5.01 and 4.71 (dd, 1 H each, 10″-H_2), 4.47 (dd, 1 H, 3″-H_b), 4.30 (br m, 1 H, 2″-H), 3.87 (dd, 1 H, 3″-H_a), 1.76 (s, 3 H, 6″-CH_3). These data immediately indicated the lack of a deoxyribose moiety in both adducts. Furthermore, each showed three sets of exchangeable signals (integrating to six total protons), which could be assigned as follows by comparison with mitosene **2b** and guanine: 6.74/6.58/6.20 ppm (**5**) and 6.59/6.38/6.22 ppm (**6**) due to 10a″-, 7″-, and 2-NH_2 groups (individual assignments not necessarily respective). The mitosene 2-NH_2 function is protonated in these adducts and thus is generally not observed due to acute broadening. The mitosene 1-H signals are observed at 5.59 (**5**) and 6.36 ppm (**6**), as compared to the ~5 ppm value, which is generally observed for simple 1-OH mitosenes [e.g., Taylor and Remers (1975)]; the large downfield shifts for the 1-H signals of **5** and **6**, in addition to the presence of intact 10a″-, 7″-, and 2-NH_2 groups, thus indicated that the guanine base moiety is linked to the mitosene skeleton at C-1.

FTIR Spectroscopy. The utility of difference FTIR spectroscopy in assigning the heterosubstitution on alkylated *guanosines* has previously been shown (Kasai et al., 1978). As shown in Figure 5A–F, the region 1800–1400 cm^{-1} contains strong absorptions that are characteristic of the substitution site on Gua derivatives. Removal of the overlapping mitosene (M) absorptions from the adduct spectra of **5** or **6** (virtually identical FTIR) was effected by weighted subtraction of the spectrum of mitosene **2b** from that of adduct **5** (Figure 6A) with the mutual mitosene ~1722-cm^{-1} carbamate peak (stippled peak) as subtraction marker (this region is devoid of G-related peaks). A comparison of this difference spectrum (Figure 6B) with those of known model alkylguanines (Figure 5) reveals a strong correlation of the adduct's guanine infrared absorptions (Figure 6B) with the spectrum of *N*7-(2-hydroxyethyl)guanine (Figure 5E; reproduced in Figure 6D); thus, the adduct appears to bear an N7-substituted guanine moiety.

A great deal of additional information can be gleaned from the absorbance FTIR spectra upon calculation of the corresponding second-derivative FTIR (SEDIR) spectra (Susi & Byler, 1983; Lee et al., 1984; Verdine & Nakanishi, 1985a; Tomasz et al., 1986a) as demonstrated in Figure 5a–f. Thus, poorly resolved shoulders in the absorbance spectra become sharp, clearly defined minima in the SEDIR spectra (compare spectra A–F with spectra a–f in Figure 5). Calculation of the second derivative of the difference spectrum in Figure 6B yields the difference SEDIR spectrum in Figure 6C. At least one additional strong IR band at 1614 cm^{-1} emerges only upon second differentiation, and this band correlates well with the 1609-cm^{-1} band exhibited by *N*7-(2-hydroxyethyl)guanine (Figure 6D/E). Thus, comparison of the difference SEDIR spectra C/E of Figure 6 reveals more detail than that of spectra B/D of Figure 6 and leads to the clear assignment of an N7-substituted guanine moiety in **5** and **6**.

UV Spectroscopy. Additional evidence for the structures of **5** and **6** comes from UV difference spectra and second-derivative UV difference (SEDUV) spectra. [A preliminary account of these methods has been published elsewhere (Verdine & Nakanishi, 1985a).] As seen in Figure 7A–F, the electronic spectra of substituted guanines differ according to the Gua heterosubstitution site. Figure 8A shows the weighted subtraction of the UV spectrum of mitosene **33** from that of

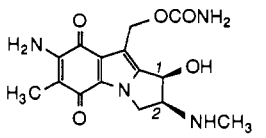

33

adduct **5** to produce the difference spectrum **5** – **33**; only poor agreement of the latter spectrum is seen upon comparison with the UV spectra of the model compounds in Figure 7A–F. This lack of correspondence is particularly due to the lack of spectral resolution, which results from the large bandwidths inherent in electronic spectra. The exact peak positions can, however, be located by calculation of the corresponding SEDUV spectra (Verdine & Nakanishi, 1985a). The SEDUV spectra in Figure 8a were scanned in the same solutions as those em-

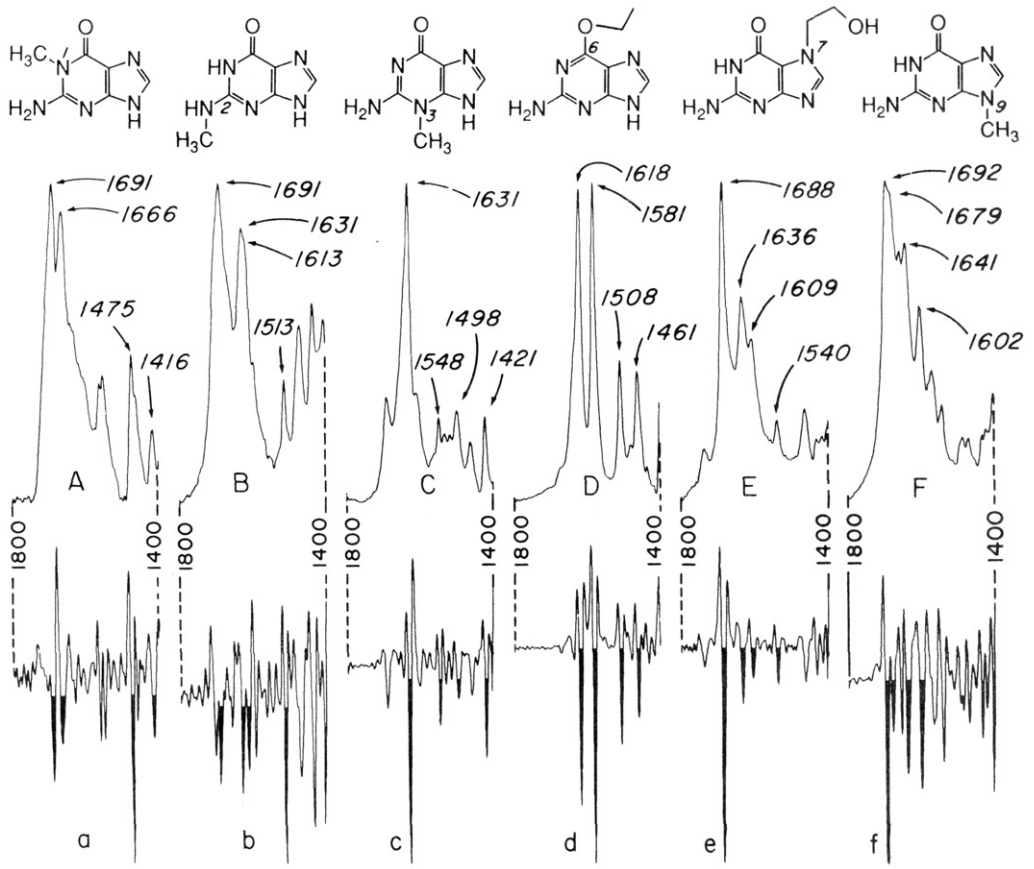

FIGURE 5: The 1800–1400-cm^{-1} region of the FTIR of guanines (Me_2SO-d_6 solution, ATR CIRCLE microcell). (A–F) Absorbance FTIR; (a–f) SEDIR. Characteristic peaks for each substitution site are indicated (cm^{-1}) in spectra A–F; corresponding SEDIR peaks are blacked out in spectra a–f.

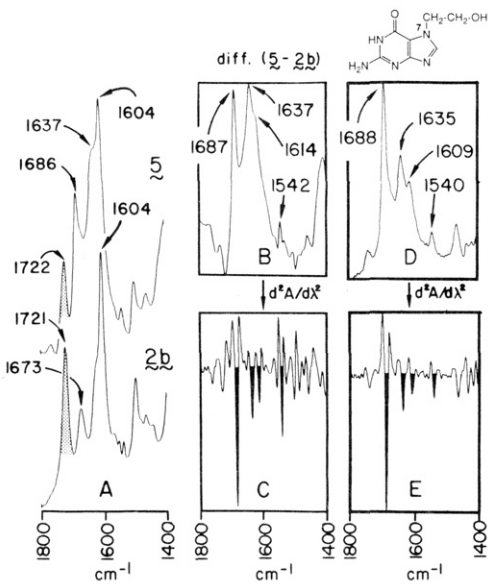

FIGURE 6: The 1800–1400-cm^{-1} region of the FTIR spectra. (A) Absorbance FTIR of M–guanine-A (**5**) and mitosene **2b**. Stippled peak denotes mutual mitosene carbamate band, which was used as a subtraction marker. (B) Difference FTIR resulting from weighted subtraction of the spectrum of **2b** from adduct **5**. (C) Second-derivative FTIR (SEDIR) of the spectrum in (B); blacked out peaks correspond to those indicated in (B) above. (D) Absorbance FTIR of *N*7-(2-hydroxyethyl)guanine reproduced from Figure 5E. (E) SEDIR of the spectrum in (D); blacked out peaks correspond to those indicated in (D) above.

ployed in the absorbance UV measurements; also, the weighted subtraction of the SEDUV spectrum of **6** from **33** was performed by using the same concentration adjustment (weighting) factor as that used in Figure 8A. [It is permissible to use multiplicative concentration adjustment (weighting) factors in order to perform weighted subtraction of second-derivative spectra, since the magnitude of $d^2A/d\lambda^2$ varies linearly with concentration (i.e., Beer's law is obeyed) in both SEDIR and SEDUV spectra [Tomasz et al. (1986a) and references cited therein].] The agreement of this difference SEDUV spectrum (Figure 8a) with the SEDUV spectrum in Figure 7e is excellent. Figure 9a shows an expanded-scale view of the SEDUV spectrum of *N*7-(2-hydroxyethyl)guanine superimposed on the adduct difference SEDUV spectrum in which the requisite comparison is readily made: 205 vs. 205 nm; 215 vs. 215 nm; 245 vs. 246 nm; 285 vs. 284 nm. Comparison of the respective absorbance spectra reproduced in expanded form in Figure 9A is not nearly as instructive. Thus, the resolution enhancement gained by calculation of SEDUV spectra permits the assignment of an N7-Gua linkage site in the M–guanines, in agreement with the results obtained in the FTIR experiments described above.

CD Spectroscopy. The remaining point of M–guanine adduct stereochemistry at C-1″ was elucidated with CD spectroscopy. The configuration of the mitosene 2″-NH_2 group is β, as all known aziridine ring opening reactions of MC occur with conservation of configuration at C-2 [cf. **2**; e.g., Kohn and Zein (1983) and references cited therein]. The problem of assigning vicinal stereochemistry in **5** and **6** thus reduces to one of adduct stereochemistry at C-1″. We have previously shown (Tomasz et al., 1983, 1984) that the sign of the Cotton effect (CE) in the ~530-nm region is unambiguously related to the configuration of the C-1 substituent; thus, a positive ~530-nm CE is associated with a 1β configuration while a negative CE is associated with a 1α configuration (cf. **2**; C-1

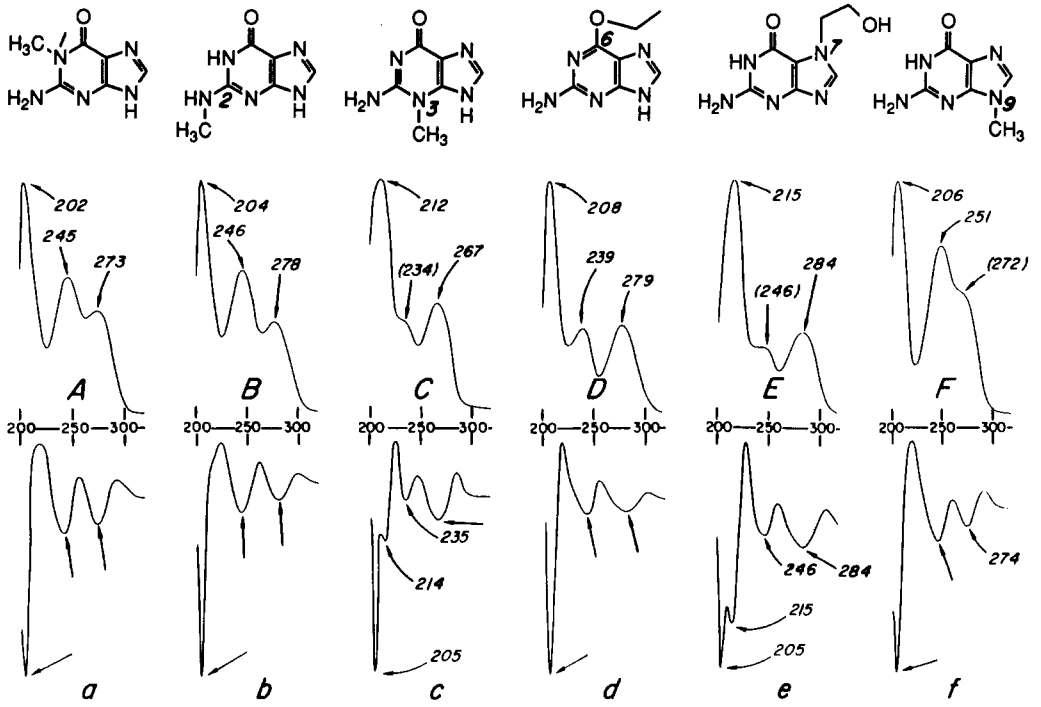

FIGURE 7: UV of guanines in 0.1 M potassium phosphate buffer (pH 7). Peak positions in nm are denoted. (A–F) Absorbance UV spectra; (a–f) second-derivative (SEDUV) spectra. Arrows in (a–f) correspond to maxima indicated above. Parenthesized numbers in (A–F) denote unclear shoulders which are clearly visible in (a–f).

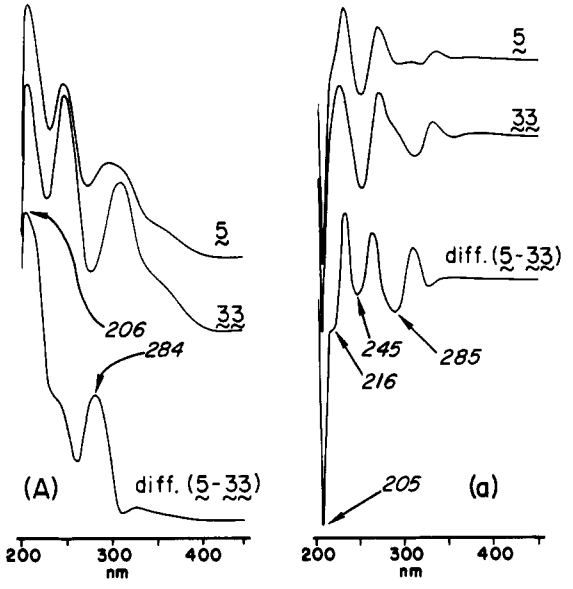

FIGURE 8: (A) UV of adduct **5** and mitosene **33** and differential spectrum of **5** – **33**. (a) SEDUV of **5** and **33** and differential SEDUV of **5** – **33**.

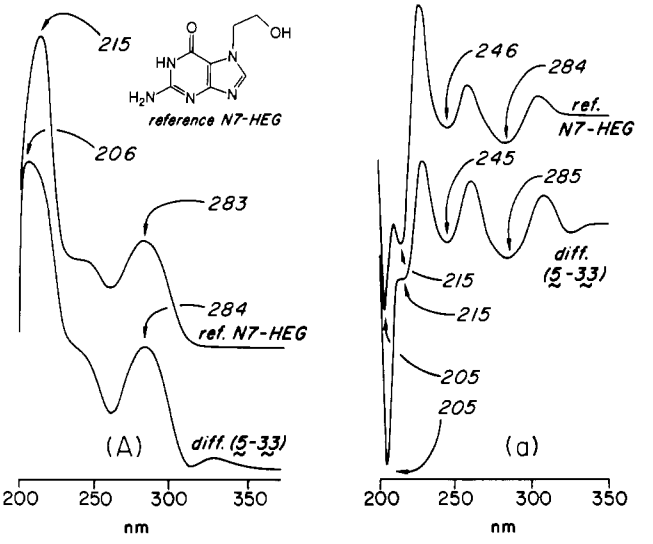

FIGURE 9: Comparison of the differential UV and SEDUV spectra of **5** – **33** with those of *N*7-(2-hydroxyethyl)guanine (*N*7-HEG). (A) Absorbance UV; (a) SEDUV.

substituent = Y). As shown in Figure 10, M–guanine **5** exhibits a CE at ~525 nm, $\Delta\epsilon = -0.081$ (hatched peak), and therefore has a 1″α configuration; **6** has a ~520-nm CE, $\Delta\epsilon = 0.112$ (hatched peak), and therefore has a 1″β configuration.

Multiple Products of the Imidazolium Ring Opening of N7-Ethyl- and N7-Methylguanosine. The original structure determination of the products of imidazolium ring opening of *N*7-alkylguanosines employed *N*7-methylguanosine (**26**) as starting material and arrived at a single structure, **27**, as the sole homogeneous reaction product (Haines et al., 1962). *N*7-Ethylguanosine (**11**) was chosen as the primary target for study here due to the fact that its ring-opened products are more readily separable than the corresponding *N*7-methyl compounds. As shown in Figure 11, the same products arise regardless of whether the *N*7-alkyl substituent is a methyl or ethyl group. *N*7-Ethylguanosine (**11**) was prepared by the reaction of ethyl iodide with guanosine (Tomasz et al., 1985). Generally, the small amounts of unreacted guanosine present in these preparations could be removed readily by passage of crude **11** through a Sephadex G-25 column (5.0 × 56 cm, 100% H_2O eluent; **11** elutes at 1100 mL). Purified **11** was treated with 2 N NH_4OH for 2 h at room temperature (Haines et al., 1962), frozen, and lyophilized to dryness. More conveniently, crude **11** (ca. 90–95%) could be hydrolyzed and the reaction mixture then chromatographed on Sephadex G-25 (conditions as above; **13**–**15** elute at 980 mL) to remove guanosine. Paper chromatography of the ring-opened product mixture with several systems as described by Haines et al. (1962) and Singer (1972) shows a single spot in all the cases of hydrolyzed **11**, **19**, and **26**, in agreement with the original reports. The mixture of products also elutes as a single band

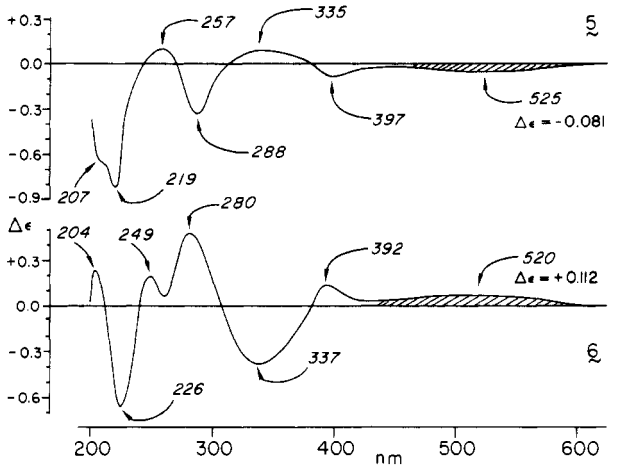

FIGURE 10: Circular dichroism (CD) spectra of M-guanine-A (**5**) and M-guanine-B (**6**) in MeOH. Hatched peaks denotes diagnostic long-wavelength Cotton effects.

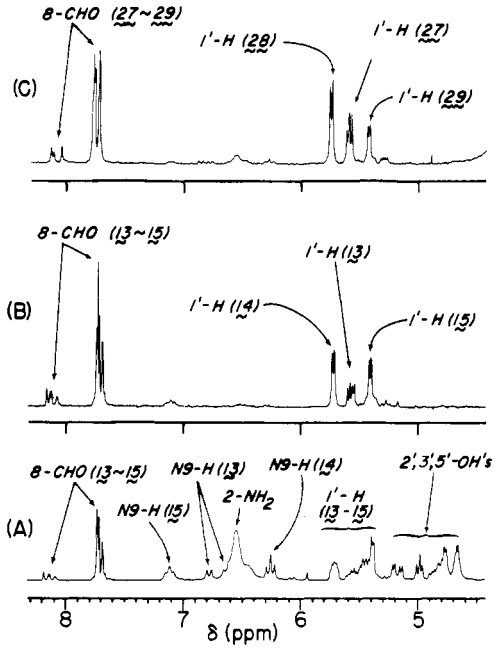

FIGURE 11: ^{1}H NMR spectra of ring-opened *N*7-alkylguanosines in Me_2SO-d_6. (A) Ring-opened *N*7-ethylguanosine (**13–15**); (B) deuterium-exchanged spectrum of ring-opened *N*7-ethylguanosine; (C) deuterium-exchanged spectrum of ring-opened *N*7-methylguanosine (**27–29**). Peak assignments are indicated.

on Sephadex G-25 (Results). HPLC (IBM-ODS, 1.0 × 25 cm; 1.5:98.5 MeCN/H_2O; 3.0 mL/min, 254-nm detection; not shown) of the Sephadex G-25 purified hydrolysis mixture gave an ill-resolved multiple peak pattern, the components of which interconverted at room temperature. ^{1}H NMR analysis (Figure 11A) showed the presence of three clusters of anomeric proton signals, all of which simplified upon deuterium exchange (Figure 11B). Separation of individual components from the mixture was effected by collection of 0.5-min HPLC fractions into a flask immersed in a dry ice–acetone bath (−78 °C) and subsequent lyophilization of the frozen sample. Reinjection of the purest fractions provided essentially homogeneous isolated samples of **13**, **14**, and **15**; retention times are 11.2, 13.2, and 10.0 min, respectively.

*N*7-Methylguanosine, **26**, was hydrolyzed (2 N NH_4OH, 2 h, 25 °C) and lyophilized, and the reaction products were analyzed by ^{1}H NMR (Figure 11C, deuterium-exchanged spectrum). Owing to the striking similarity of spectra B and C of Figure 11, it can be concluded that the hydrolysis products

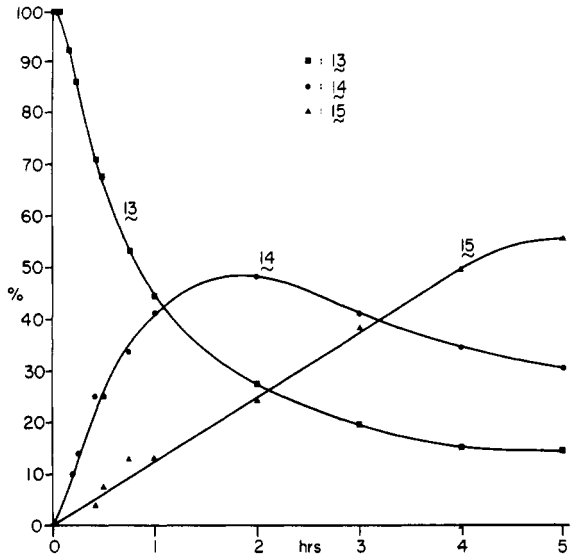

FIGURE 12: Kinetic study of the products arising from basic hydrolysis of *N*7-ethylguanosine (**11**).

of **26** bear the same rearranged sugar moieties as those generated from hydrolysis of **11**. Furthermore, comparison of the ^{1}H NMR spectra of *N*7-ethyl-FAPyr triacetates **16–18** [below and Tomasz et al. (1985)] with those of *N*7-methyl-FAPyr triacetates **30–32** reveals that the respective members of each series display very similar proton resonances, with the exception of the *N*7-alkyl substituent signals.

Kinetic Study of the Basic Hydrolysis of N7-Ethyl- and N7-Methylguanosine (**11** *and* **26**). Pseudo-first-order rate constants of 6.25 × 10^{-2} min^{-1} (**11**) and 2.41 × 10^{-2} min^{-1} (**26**) were observed, corresponding to half-lives of 11.1 and 2.9 min, respectively. The product distribution of **11–13** over time was gauged by integration of the ^{1}H NMR anomeric proton signals of each isomer present in the hydrolysis mixture upon sampling at regular time intervals. Total isomer percentages were normalized to 100% in order to correct for unreacted **11**. The results are shown in Figure 12. Several notable features are as follows: (i) the initial product arising from the hydrolysis of **11** is essentially a single compound, **13** (Scheme II), which slowly gives rise to the isomers **14** and **15**; (ii) **14** is formed more rapidly than **15**, and it is the predominant product from ca. 1.1 to 3.2 h (its formation kinetics suggest that **14** is the kinetic product of the reclosure of imine **12**); (iii) at longer time intervals (after about 3.2 h), pyranoside **15** predominates; (iv) the relative product ratios level off after ~5 h to a value of ca. 1.0 (**13**):2.4 (**14**):4.0 (**15**) (such equilibration suggests that the ratios obtained at >5 h are reflective of the relative thermodynamic stabilities of the three riboside isomers); (v) comparison of the kinetics of disappearance of **11** with those of product equilibration suggests that the formation of imine **12** does not occur directly from **11** (i.e., concerted imidazolium cleavage/sugar opening does not occur), but rather **12** is initially formed from **13** and later from **13–15** (imidazolium cleavage is much faster than formation of **12**). At reaction times >5 h, interfering peaks appear that are probably due to the presence of free ribose (formed by the hydrolysis of imine **12**), precluding accurate integration of ^{1}H NMR signals. As a result of this study, a simplified procedure for the isolation of pure **13–15** emerges. Thus, hydrolysis of **11** for 5 min followed by HPLC (as above) yields **13** as the sole product (ca. 30% yield); at 1.75 h, **14** is the predominant product (ca. 45%) and is more readily isolated by HPLC at that time; at 5 h, **15** predominates (ca. 55%) and can then be readily obtained in pure form.

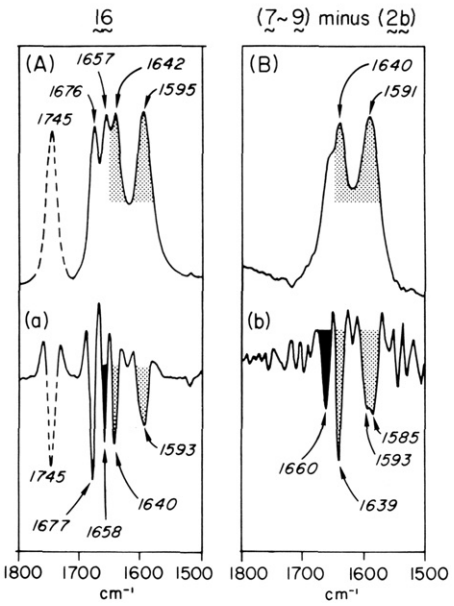

FIGURE 13: The 1800–1500-cm^{-1} region of the FTIR (Me_2SO-d_6 solution, ATR CIRCLE microcell). (A/a) Spectrum of (*N*7-ethyl-FAPyr)-β-ribofuranose triacetate **16**; (B) weighted difference spectrum of M–dG_I (mixture of **7–9**) minus mitosene **2b**; (a/b) SEDIR spectra corresponding to (A/B), respectively. Stippled peaks in (A/B) and (a/b) denote common absorptions that are visible before second differentiation; blacked-out peaks in (a/b) denotes absorption that can only be clearly discerned after second differentiation. Dashed peak in (A/a) corresponds to the acetate carbonyl stretching band and is not relevant to the comparison of **16** and **7–9**.

Acetylation of **13–15** *and Structure Determination of N7-Ethyl-FAPyr Compounds* **16–18**. Pure samples of **13–15** were acetylated individually and purified by HPLC (Methods) to yield the respective triacetates **16–18**. Acetylation was performed in order to (i) assess the positions of free hydroxyl groups on each isomer and thereby assign the sugar structure and (ii) furnish derivatives that are soluble in some polar organic solvents (MeOH and Me_2CO) and are therefore more suitable for detailed ^{1}H NMR measurements (see below). Pure **13–15** underwent no ribose rearrangement during the acetylation process; thus, preparative-scale acetylation of the crude mixture of **13–15** followed by TLC/HPLC separation (Methods) of the triacetates **16–18** was employed in order to obtain the latter in homogeneous, milligram quantities.

Acetates **16–18** gave virtually identical UV spectra: in MeCN, 211, 238 (sh), and 272 nm; in MeOH, 216 (ε 32 000), 242 (sh, ε 3700), and 276 (ε 12 500) nm. The UV spectra for **16–18** are typical for *N*7-alkyl-FAPyr compounds (Singer & Grunberger, 1983). Compounds **16–18** gave mass spectral molecular ions of m/z 456 (M + 1, CI-MS, CH_4 carrier gas). In addition, the 1800–1500-cm^{-1} FTIR spectra (Figure 13A/a) of **15–18** are identical, thus establishing that they bear identical *N*7-alkyl-FAPyr bases. ^{1}H NMR showed the following: (**16**) see Figure 14; (**17**) δ 10.76 (exch br s, 1 H, N1-H), 8.28/8.27 (two s, 8-CHO minor rotamers), 7.81/7.78 (two s, 8-CHO major rotamers), 7.04/6.86 (two exch br s, 2 H, 2-NH_2 major and minor rotamers, respectively), 6.13/6.09 (two overlapping dd, 1 H, 1′-H major rotamers), 5.84/5.67 (two exch d, N9-H major rotamers), 5.56/5.47 (two exch d, N9-H minor rotamers), 5.32–5.15 (m, 2 H, 2′- and 3′-H's), 4.27–4.02 (m, 3 H, 4′- and 5′-H_2's), 3.62–3.19 (m, 2 H, N7-CH_2CH_3), 2.06, 2.04, and 2.00 (three s, 9 H, acetate CH_3's), 1.05 and 1.02 (two t, 3 H, N7-CH_2CH_3); (**18**) δ 10.67 (exch br s, 1 H, N1-H), 8.31/8.28 (two s, 8-CHO minor rotamers), 7.90/7.80 (two s, 8-CHO major rotamers), 6.75/6.61 (exch br s, 2 H, 2-NH_2 major and minor rotamers, respectively), 6.18/6.05 [two exch d, 1 H, N9-H major rotamers (overlap minor rotamers)], 5.80/5.78 (two overlapping dd, 1 H, 1′-H major rotamers), 5.55 (dd, 1 H, 3′-H), 5.10/5.09 (two overlapping dd, 1 H, 2′-H), 4.97 (m, 1 H, 4′-H), 3.7–3.2 (m, 4 H, 5′-H_2 and N7-CH_2CH_3), 2.10, 1.98, and 1.95 (three s, 9 H, acetate-CH_3's), 1.01/0.99 (two t, 3 H, N7-CH_2CH_3 minor and major rotamers, respectively). Examination of the chemical shift values for the 2′-, 3′-, 4′-, and 5′-proton signals for **16–18** provided directly the assignment of ribofuranose triacetate for the sugar portions of **16** and **17**, as well as that of pyranose triacetate for **18**. Specifically, the 2′- and 3′-protons of **16** and **17** are found below 5 ppm while the 4′- and 5′-proton signals coincide at 4.3–3.9 ppm, consistent with the presence of acetate esters at the 2′-, 3′-, and 5′-positions (i.e., ribofuranose triacetate); in **18**, the 2′-, 3′-, 4′-, and 5′-proton signals are observed at ~5.1, 5.6, 5.0, and 3.7–3.5 ppm, respectively, consistent with the presence of acetate esters at the 2′-, 3′-, and 4′-positions (ribopyranose triacetate). NOE experiments conducted on each isomer established the respective 1′ configurations; relevant NOE enhancements are indicated in partial structures **16a**, **17a**, and **18a**.

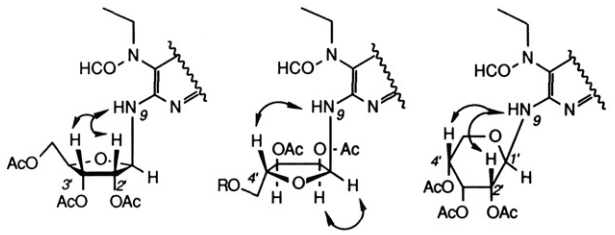

N7-Alkyl-FAPyr Ribosides Exist as a Set of N-Formyl Rotamers. The ^{1}H NMR spectrum of *N*7-ethyl-FAPyr 1′β-ribofuranose triacetate **16** is shown in Figure 14. The spectra of *N*7-methyl-FAPyr riboside triacetates **30–32**, Me_2SO-d_6 solvent, are as follows: (**30**) δ 10.65 (exch br s, 1 H, N1-H), 8.06 (s, 8-CHO minor rotamers), 7.70/7.69 (two s, 8-CHO major rotamers), 7.45/7.37 (two exch d, N9-H major rotamers), 7.03/6.99 (two exch d, N9-H minor rotamers), 6.63/6.54 (two exch br s, 2-NH_2 major and minor rotamers, respectively), 5.88/5.79 (two dd, 1 H, 1′-H), 5.35/5.32 (two dd, 1 H, 2′-H) 5.24/5.22 (two dd, 1 H, 3′-H), 4.28–4.15 (m, 1 H, 4′-H), 4.05–3.92 (m, 2 H, 5′-H_2), 2.88/2.85 (two s, N7-CH_3 minor rotamers), 2.77/2.75 (two s, N7-CH_3 major rotamers), 1.99 and 2.03 (two s, 9 H, acetate CH_3's); (**31**) δ 10.88 (exch br s, 1 H, N1-H), 8.18 (two s, 8-CHO minor rotamers), 7.81/7.77 (two s, 8-CHO major rotamers), 6.69/6.85 (two exch br s, 2 H, 2-NH_2 major and minor rotamers, respectively), 6.10/6.07 (two dd, 1 H, 1′-H), 5.90/5.79 [two exch d, 1 H, N9-H major rotamers (minor rotamers not visible], 5.30–5.13 (m, 2 H, 2′- and 3′-H), 4.32–4.00 (m, 3 H, 4′-H and 5′-H_2), 3.02/2.96 (two s, N7-CH_3 minor rotamers), 2.87/2.80 (two s, N7-CH_3 major rotamers), 2.04, 2.02, and 2.00 (three s, 9 H, acetate CH_3's); (**32**) δ 11.25 (exch br s, 1 H, N1-H), 8.21/8.18 (two s, 8-CHO minor rotamers), 7.88/7.80 (two s, 8-CHO major rotamers), 7.04/6.85 (two exch br s, 2 H, 2-NH_2 major and minor rotamers, respectively), 6.15/6.07 [two exch d, N9-H major rotamers (minor rotamers not separated)], 5.79/5.77 (two dd, 1 H, 1′-H), 5.54/5.53 (two dd, 1 H, 3′-H), 5.08/5.06 (two dd, 1 H, 2′-H), 4.97/4.94 (two dd, 1 H, 4′-H), 3.5–3.8 (m, 2 H, 5′-H_2), 3.05/2.97 (two s, N7-CH_3 minor rotamers), 2.93/2.83 (two s, N7-CH_3 minor rotamers), 2.02, 2.00, and 1.97 (three s, 9 H, acetate CH_3's).

In the spectrum of **16** (Figure 14), it can be seen that the resonances corresponding to 1′-H, 2′-H, and 3′-H appear as

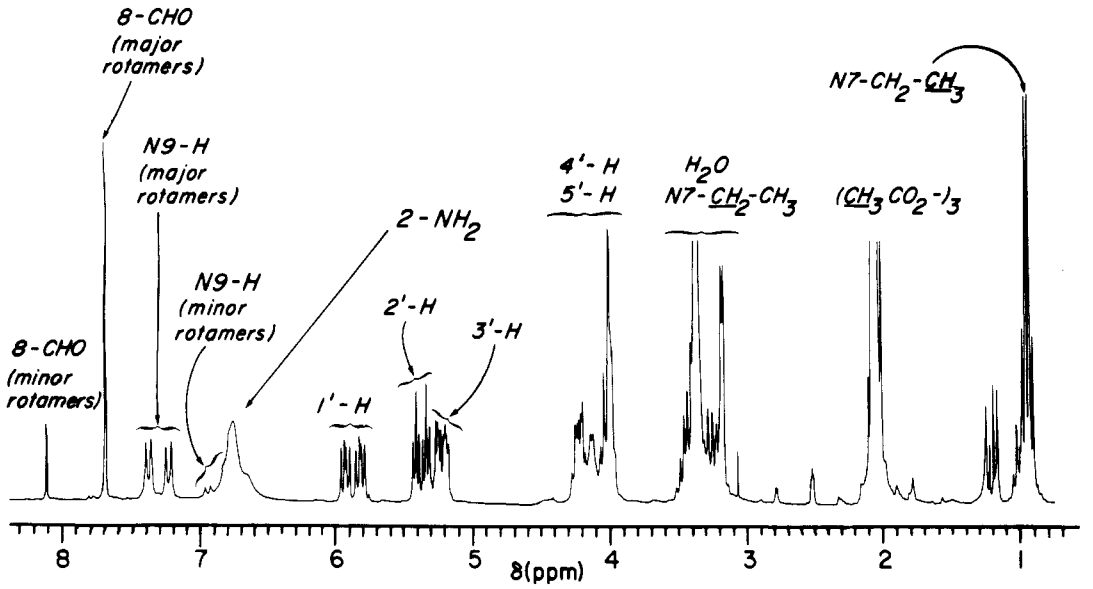

FIGURE 14: The 8.4–0.7 ppm region of the ^{1}H NMR of **16** in Me_2SO-d_6. Assignments are indicated.

a set of two discreet multiplets with almost identical proton–proton coupling constants. The integral peak area ratio of the 1′H signals at 5.93 and 5.82 ppm is ~1:1. However, the 8-CHO gives rise to two apparent signals at 8.12 and 7.70 ppm with an integral peak area ratio of ~1:8. This apparent discrepancy in integral ratios is reconciled by the observation that the *N*-formyl proton signals in the corresponding *N*7-methyl FAPyr triacetate **30** as well as isomers **17** and **18** appear as *four* signals in a ratio of about 1:1:8:8. In most cases studied here, the *N*-formyl protons of *N*7-alkyl-FAPyr ribosides are manifest as a set of two resolved low-intensity signals at 8.5–8.0 ppm and a set of two resolved high-intensity signals at 8.0–7.5 ppm; the sets are usually separated by >0.3 ppm. Thus in **16**, coalescence of the two signals within each set results in observation of only one signal each for the high- and low-field *N*-formyl resonances. Further evidence for this assertion comes from the observation of four N9-H peaks in the ^{1}H NMR spectrum of **16** (Figure 14); two are at 6.95 and 6.82 ppm (minor), and two are at 7.39 and 7.24 ppm (major) (ratio ~1:1:8:8). Thus, triacetate **16** and all other *N*7-alkyl FAPyr compounds studied here exist as an assemblage of four *N*-formyl rotamers; of these four, two are predominant and approximately equal in population ("major rotamers"; 8-CHO <8 ppm) while two are present to an extent of ~15% and are also approximately equal in population with respect to each other ("minor rotamers"; 8-CHO >8 ppm). The appearance of a set of two 1′-H multiplets in a 1:1 ratio is probably due to one major and one minor rotamer in each multiplet. All attempts at chromatographic separation of these rotamers have failed. The presence and interconversion of *N*-formyl rotamers has been previously observed in similar systems (Boiteux et al., 1984; Discussion).

Structures of the Products Formed in Alkaline Hydrolysis of N7-Methyl-2′-deoxyguanosine (**19**). Model compound **19** was hydrolyzed and the reaction worked up by the same procedure as that used for the hydrolysis of **11** and **26**. ^{1}H NMR of the crude hydrolysis mixture revealed the presence of at least three 1′-H signals at 6.01, 5.90, and 5.35 ppm which simplified upon the addition of MeOH-d_4 (Figure 15A). The crude mixture was acetylated as above and subjected to HPLC (IBM-ODS, 1.0 × 25 cm; 16:84 MeCN/H_2O; 3.0 mL/min, 254-nm detection). On HPLC (not shown), a broad elution envelope resulted, with discernible peaks at 11, 14, and 16 min,

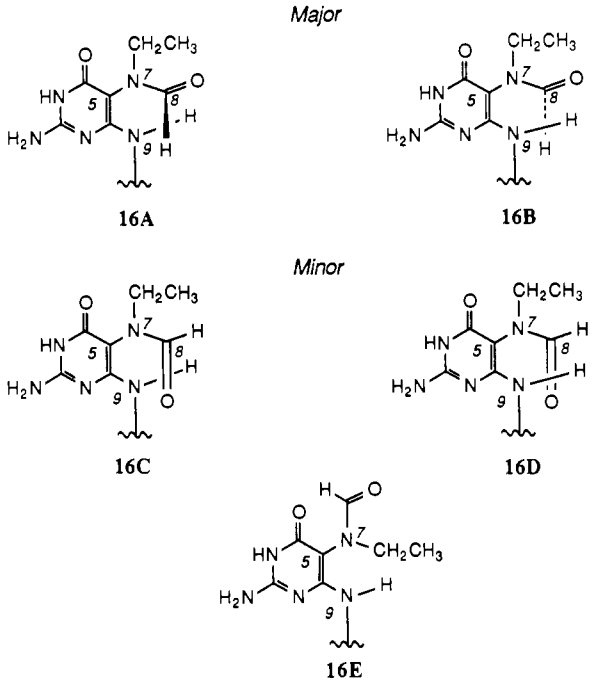

designated A, B, and C, respectively. Compound **25** was isolated in homogeneous form by repeated fractionation of crude fraction A. Reinjection of peaks B or C regenerated the **23**/**24** mixture under all conditions attempted; thus compounds **23** and **24** were inseparable. The ^{1}H NMR spectra of **23** and **24** (as a mixture) and **25** are as follows: (**23**/**24**) δ 10.37/10.34 (exch br s, 2 H, N1-H's), 8.10/8.07/8.05/8.03 (four s, 8-CHO's minor rotamers), 7.75/7.70/7.67 (three s, 8-CHO's major rotamers), 7.06/6.99 (two exch d, 1 H) and 6.63/6.52 (two exch d, 1 H) (N9-H's), 6.58 (exch br s, 4 H total, 2-NH_2's), 6.05/5.97 (two ddd, 1 H each, 1′-H's), 5.07/5.00 (two ddd, 2 H, 3′-H's), 4.2–3.8 (m, 6 H, 4′-H's and 5′-H_2's), 2.78/2.77/2.75 (three s, 6 H total, N7-CH_3's), 2.45/2.15 (two m, 4 H, 2′-H's), 2.03 (s, 12 H, acetate CH_3's); (**25**) δ 10.34 (exch br s, 1 H, N1-H), 8.03/7.95 (two s, 8-CHO minor rotamers), 7.76/7.72 (two s, 8-CHO major rotamers), 7.32 and 7.21 [two exch d, 1 H, N9-H major rotamers (minor rotamers not visible)], 6.50 (exch br s, 2 H, 2-NH_2), 5.34 (ddd, 1 H, 1′-H), 5.04–4.91 (m, 2 H, 3′- and 4′-H), 3.79/3.56 (dd, 2 H, 5′-H_2), 2.94/2.87 (two s, N7-CH_3 minor rotamers),

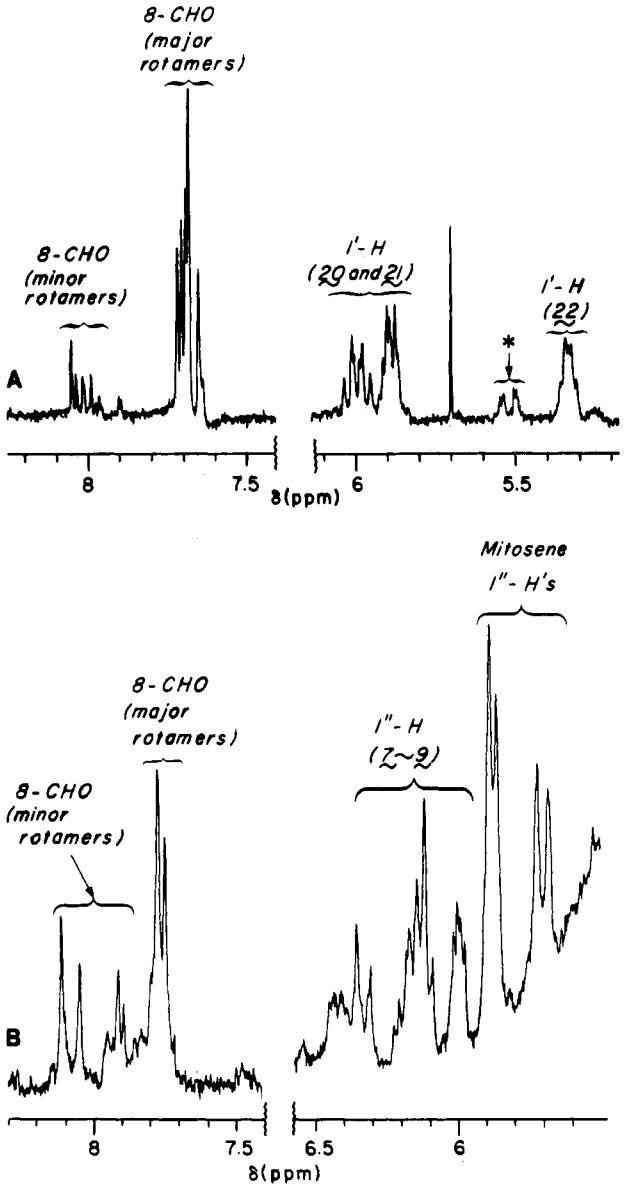

FIGURE 15: Downfield region of the ^1H NMR spectra in Me_2SO-d_6; assignments are as given. (A) Mixture resulting from the hydrolysis of *N*7-methyl-2′-deoxyguanosine (**19**); asterisk denotes a minor unknown compound that may be 1′α-**22**. (B) M–dG_I (mixture of **7–9**).

2.80/2.74 (two s, N7-CH_3 major rotamers), 2.32/1.70 (two m, 1 H each, 2′-H_2), 2.06/1.94 (two s, 6 H, acetate CH_3's). Despite the inseparability of **23** and **24**, it is possible to conclude on the basis of ^1H NMR measurements that the **23**/**24** mixture consists of the 1′α- and 1′β-anomers of 2′-deoxyribose 3′,5′-diacetate linked to an *N*7-methyl-FAPyr base. On the other hand, **25** possesses a 2′-deoxyribopyranose 3′,4′-diacetate sugar linked 1′β to the *N*7-methyl-FAPyr base. Thus, it appears that the analogous set of three *N*7-alkyl-FAPyr compounds are produced upon hydrolysis of *N*7-alkylguanosines and *N*7-alkyl-2′-deoxyguanosines.

Properties of M–dG_I: A Mixture of Interconverting Components. The M–dG_I adduct fraction from Sephadex G-25 chromatography (Figure 1B) was subjected to HPLC (Methods; Figure 2), and four fractions were collected at room temperature as indicated by the numbering in Figure 2A. Upon reinjection of any of the four peak fractions, an HPLC elution profile resulted that contained all of the components present in the initial chromatographic separation; thus, M–dG_I is a mixture of components that interconvert among each other on the HPLC time scale at room temperature. The rate of

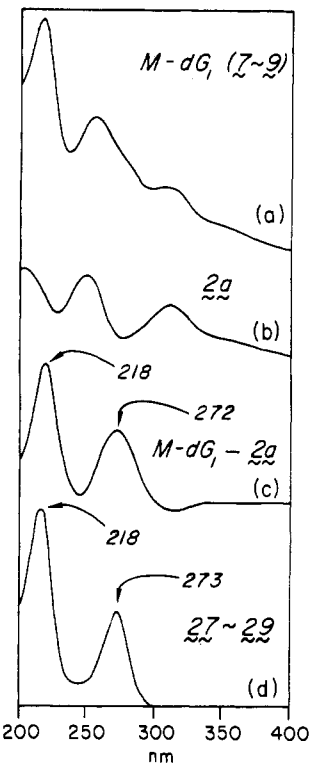

FIGURE 16: (a) UV spectra of M–dG_I (mixture of **7–9**) and (b) mitosene **2a**; (c) weighted difference spectrum of (M–dG_I minus **2a**); (d) UV spectrum of ring-opened *N*7-methylguanosine (**27–29**). Peak positions are indicated in nm.

interconversion was observed to be highest for fractions 3 and 4 (Figure 2A), since reinjection of either of these fractions immediately following collection regenerated essentially the original pattern (Figure 2B). Similar reinjection of peaks 1 and 2 (Figure 2A) showed the presence of all four peaks only after several hours at room temperature. The UV spectra of the isolated fractions were essentially identical with one another whether measured in the HPLC solvent immediately after collection or at three different pH values (2, 7, and 10) after desalting and lyophilization. Figure 16 shows a representative spectrum of M–dG_I measured at pH 7.

Difference UV Spectra of M–dG_I. Weighted subtraction of the UV spectrum of **2a** from that of M–dG_I was performed at pH 2, 7, and 10. In each case, a difference spectrum resulted that was extremely close to that of ring-opened *N*7-methylguanosine (**27–29**, see below) in the same solvent, suggesting that the Gua-derived chromophore of M–dG_I is identical with the base moiety of ring-opened *N*7-ethylguanosine. Additional absorption maxima data for the difference UV experiments at several pH values are as follows: (i) in 0.01 N HCl (pH 2), **27–29**, 272 and 216 nm, M–dG_I difference spectrum, 270 and 217 nm; (ii) in 0.01 N NaOH, **27–29**, 265 nm, M–dG_I 265 nm.

Perchloric acid hydrolysis of M–dG_I yielded no guanine, indicating the absence of an intact guanine base moiety in M–dG_I.

C-1″ stereochemistry of M–dG_I was elucidated by CD spectroscopy as detailed above for the M–guanines. As all of the components of M–dG_I (**7–9**) interconvert on HPLC, all of them must possess the same 1″ stereochemistry; epimerization of the mitosene 1″-position is ruled out under the neutral HPLC conditions employed here. The mixture of **7–9** gives rise to a weak positive CE at ~550 nm (not shown), and the C-1″ stereochemistry is thus β in all components.

Structures of the Constituents of M–dG$_I$. As mentioned above, subtraction of the UV spectrum of mitosene **2a** from that of M–dG$_I$ (**7–9**) generates a difference UV spectrum that is nearly identical with the UV spectrum of ring-opened *N*7-methylguanosine (mixture of **27–29**; Figure 16), thus indicating that M–dG$_I$ posesses the same *N*7-alkyl-FAPyr base moiety as that present in **27–29**. Further proof is afforded by differential FTIR measurements. Figure 13 shows (spectrum B) the 1800–1500-cm^{-1} region FTIR of M–dG$_I$ (mixture of **7–9**) after weighted subtraction of the mitosene-related FTIR absorptions (same protocol as above) and (spectrum A) the FTIR of *N*7-ethyl-FAPyr triacetate **16**. The hatched and blacked-out peaks in spectra A/B and a/b of Figure 13 correspond to FTIR absorptions that are common to both spectra; it is clear that there is significant similarity in the FAPyr base moiety of M–dG$_I$ and **16**. Furthermore, comparison of the corresponding SEDIR spectra in Figure 13a/b reveals that all three *N*7-alkyl-FAPyr-related FTIR absorptions in the adduct difference spectrum agree extremely well with the pyrimidine absorptions exhibited by **16**. The resolution of the spectrum in Figure 13b is sufficiently high that identification of the obscured peak at 1660 cm^{-1} in Figure 13A is readily achieved (compare spectrum b, blacked-out peak, and spectrum B, shouldered peak).

One significant difference, however, between the adduct difference spectra (Figure 13B/b) and the model spectra (Figure 13A/a) is the presence of a ~1676-cm^{-1} absorption in the latter which seems to be absent in the former. As the 1677-cm^{-1} peak is assignable to the *N*-formyl group in **16**, one would expect to see the corresponding *N*-formyl FTIR absorptions in the spectra of M–dG$_I$. The probable cause of this discrepancy lies in the fact that M–dG$_I$ bears an ammonium group (mitosene 2″-NH$_2$ group is protonated) in close proximity to the formamide nitrogen whereas **16** contains a simple ethyl group; thus one could envision interaction of the ammonium and formamide functions through hydrogen-bonding or dipolar electrostatic effects. Such interactions would have a noticeable effect on the frequency and/or intensity of the formamide C=O absorption, thus rendering it unobservable due to overlap with other peaks under the present FTIR conditions.

As evidenced by ^{1}H NMR of the **7–9** mixture (Figure 15B), the components of M–dG$_I$ do indeed possess *N*-formyl groups, judging by the presence of multiple singlet nonexchangeable peaks in the region 8.2–7.7 ppm. In analogy to all other *N*7-alkyl-FAPyr ribosides described here, M–dG$_I$ displays multiple 8-CHO low-intensity signals at 8.2–7.85 ppm and multiple high-intensity signals at 7.85–7.7 ppm; however, in the case of M–dG$_I$ the chemical shift dispersion and intensity differences of the two sets are not as great as those observed for the hydrolysis products of *N*7-alkyl models **11**, **19**, and **26**. Evidence for the presence of multiple rearranged sugar moieties in **7–9** is gained from the observation of at least three (and possibly four) multiplet ^{1}H NMR peaks in the region 6.5–5.9 ppm corresponding to sugar anomeric 1′-H's (Figure 15B).

Thus, by analysis of the chemical degradation products of *N*7-alkylguanosines and *N*7-alkyl-2′-deoxyguanosines, it is possible to conclude by analogy that *M–dG$_I$ consists of a series of ring-opened N7-mitosenyl-2′-deoxyriboside isomers* **7–9** *which are capable of both chemical and rotameric interconversion.*

Observation of a New and Diagnostic Maximum in the UV Spectra of Ring-Opened N7-Alkylguanosines. The UV spectra of *N*7-alkyl-FAPyr ribosides [e.g., Haines et al. (1962), Singer (1972), and Singer and Grunberger (1983)] have not previously been reported below 220 nm. We have measured the UV spectra of *N*7-ethyl-FAPyr compounds **13–15**, **20–22**, and **27–29** in pH 7 H_2O; in each case, a strong UV maximum at 218 nm was observed. Conversely, a comparable absorption peak was not observed in *guanosines* alkylated at the N1- (no maximum below 220 nm), N^2- (no maximum below 220 nm), O^6- (210 nm), or N7-positions (206 nm). In addition, the M–dG$_I$ difference spectrum in Figure 16 also displays this diagnostic peak. We expect that this characteristic UV maximum will be of general use in identifying ring-opened *N*7-alkyl-FAPyr nucleosides.

Yields and Distribution of MC–Guanine Adducts. Shown in Table I are the yields and product distributions of MC–guanine adducts obtained under a variety of activation conditions and with several guanine-containing substrates.

Discussion

This work presents the production, isolation, and structure determination of a series of new mitomycin C–guanine adducts (**5–9**), all of which arise from initial covalent attachment of the mitosenyl group to the N7-position of Gua residues. Owing to this common structural feature, we postulate that all of the N7 adducts described in this paper arise from a common, unstable intermediate, **10** (Scheme I), which is inisolable under the present conditions. Namely, we propose that **10** decomposes to the observed adducts **5–9** through two different degradation pathways: (1) **5** and **6** arise via cleavage of the glycosidic bond in intermediate **10**, and (2) **7–9** are produced as a result of fission of the imidazolium ring of **10**. The imidazolium fission process initially gives rise to adduct **7**, which undergoes deoxyribose equilibration to generate the observed products **7–9** in a thermodynamically determined ratio (Scheme I). As seen in Table I (entry B), **5–9** are the predominant adducts formed in the reaction of dinucleoside phosphate d(GpC) and MC in the presence of mild acid catalysis.

Acidic vs. Reductive Activation. In contrast to the present findings, MC^{*H} has been shown previously to react with d(GpC) selectively at the N^2-position of Gua; thus, adducts **3** and **4** are produced in the latter reductive reaction to an extent of >85%, while <15% of N7 adducts (**7–9**) are observed (Figure 1B, dotted line; Table I, entry A; Tomasz et al., 1983, 1984, 1986a).[4] A similar positional selectivity depending on the activation conditions is also observed with other Gua-containing substrates, namely, deoxyguanosine and DNA [Table I, entries D/I (reductive) and E/F/H (acidic)]. Interestingly, the selectivity properties of differentially activated MC are somewhat altered by the local environment of Gua residues in DNA. Thus, MC alkylates *exclusively* the Gua-N^2 position in DNA under reductive catalysis (Table I, entry I; Tomasz et al., 1970, 1986b), indicating a remarkable enhancement in position selectivity from 85% N^2 adducts [d(GpC) substrate] to essentially 100% (DNA). MC^{*+}, however, reveals a deterioration in positional selectivity with regard to DNA alkylation. Thus, in the present work, we determined that MC^{*+} prefers to alkylate the Gua-N7 in d(GpC) and deoxyguanosine (~95% Gua-N7:~5% Gua-N^2); conversely, the reaction with DNA gives rise to ~1:1 Gua-N7/Gua-N^2 adducts (Table I).

The differential reactivity of MC under differing activation conditions may be explained as follows. The putative reactive MC^{*+} species, **34**, formed upon treatment of MC with mild acid appears to have considerable carbocationic character (Tomasz et al., 1984; McClelland & Lam, 1985). The positive charge of **34** at C-1 is not expected to be appreciably delo-

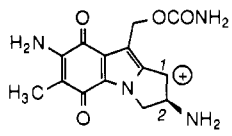

34

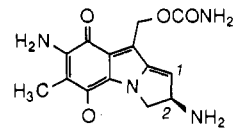

35

calized because the quinone system exerts an electron-withdrawing effect; delocalization is restricted to the C-1/C-9/N-4 pyrrole benzylic carbocation resonance structures, none of which are predicted to be stable. Consequently, **34** is a "hard" alkylating agent and should thus react preferentially with the site of highest electron density in Gua, i.e., N7 (Pullman & Pullman, 1981); analogous hard DNA alkylators include dimethyl sulfate, alkylnitrosoureas, and mustards (Singer & Grunberger, 1983). On the other hand, current evidence suggests that the reactive MC species formed upon reduction is quinone methide **35**, in which the electropositive character at C-1 is highly delocalized (Moore, 1977; Tomasz & Lipman, 1981); **35** is therefore characterized as a "soft" DNA alkylator. Other highly delocalized electrophiles such as those formed from polyaromatic hydrocarbon diol epoxides, 8-(bromomethyl)benz[*a*]anthracene, safrole, and estragole are well-known for their preferred attack at Gua-N^2 (Singer & Grunberger, 1983).

However, it was noted above that while **34** seems to exert its intrinsic preference for the N7-position of simple Gua-containing substrates [d(GpC) and dG], alkylation of DNA by **34** is not nearly as positionally selective. This difference may be due to steric hindrance of attack on the Gua-N7 atom in the DNA major groove. Thus, while attack at Gua-N7 is preferred, steric accessibility factors lead to a significant proportion of the alkylation events occurring at the more accessible nucleophile, i.e., Gua-N^2 in the minor groove. In simple monomeric nucleotides and nucleosides in general, however, the N7-atom is much more accessible, and therefore **34** is free to exert its intrinsic electronic preference for alkylating Gua-N7 almost exclusively. Thus, although the observed binding preferences of **34** and **35** are generally consistent with the DNA-alkylating properties of electronically similar species, dramatic attenuation of the intrinsic N7-Gua preference of **34** is observed in the present case, depending upon its steric accessibility in the Gua-containing substrate.

Another stereochemical feature of the alkylation of DNA by MC^{*+} deserves comment. A measurable amount of M–guanines **5** and **6** is released spontaneously from MC-alkylated DNA; the ratio of the two as eluted from Sephadex G-100 chromatography is ~1.5:1, respectively (Figure 3a). In contrast, enzymatic digestion of the remaining, partially depurinated MC–DNA complex results in the release of additional **5** but no detectable amounts of **6**. Thus, it appears that the incidence of glycosidic bond cleavage in DNA-bound **6** is much greater than that for DNA-bound **5**. An explanation for the two apparently distinct stages of release and the observed differences in product stereochemical distribution is as follows. Under the low pH conditions of the reaction of MC, local denaturation of some regions of the DNA probably occurs. Modification of denatured DNA by MC may differ from that of native DNA in the following ways: (1) The Gua-N7 position in locally denatured DNA may be sufficiently accessible as to allow facile MC alkylation by electrophile **34** from both the 1α and 1β faces, thus giving rise to 1″α-**10c** (precursor to **5**) and 1″β-**10c** (precursor to **6**). Molecular modeling experiments (unpublished results) have indicated that 1″β-**10c** is significantly more congested than 1″α-**10c** in double-stranded DNA; on the other hand, both adducts appear to fit single-stranded DNA well. Thus, both 1″α- and 1″β-isomers of **10c** are presumably formed in similar amounts in locally denatured DNA owing to the presence of a less sterically demanding template. (2) Hydrolytic release of **5** and **6** from **10c** in denatured DNA is probably much faster than that which occurs in native regions (i.e., similar to the rate of deribosylation of **10a** and **10b**). (3) Owing to the instability of 1″β-**10c** relative to 1″α-**10c** in double-stranded DNA, it is reasonable to propose that the driving force for deribosylation of the former is much greater than that of the latter, since adduct 1″β-**10c** (precursor to **6**) appears to bear a more torsionally strained glycosidic bond than 1″α-**10c** (precursor to **5**). The arguments detailed above indicate that the early-released M–guanine fraction originates from denatured DNA and consists of both stereoisomers **5** and **6**; in contrast, the late-released fraction originates from native (albeit partially depurinated) DNA in which only the 1″α-isomer of **10c** is stably incorporated for steric reasons; loss of DNA-bound **3** from the MC–DNA complex is not expected (and not observed) as previous studies have shown this adduct to be stable in DNA (Tomasz et al., 1986b).

Significance of Acidic Activation of MC in Vivo. The finding that MC forms covalent DNA adducts *under nonreducing conditions* as described here is of considerable interest because it raises the possibility that such a process occurs in vivo and may therefore be responsible for some of the observed biological properties of MC. Although enzymatic systems capable of reducing MC exist in both bacterial (Iyer & Szybalski, 1964) and mammalian cells (Schwartz et al., 1963; Kennedy et al., 1982; Tomasz & Lipman, 1981; Keyes et al., 1984; Pan et al., 1984), bioreductive alkylation may not be the only operative mechanism for the bioactivation of MC's DNA-alkylating function. The mildly acidic conditions used here may mimic the lower pH found in gastric and solid tumors, for which MC is an effective treatment (Douglass et al., 1984). This speculation is lent further support by the recent finding that the toxicity and DNA cross-linking activity of MC in aerobic EMT tumor cells are increased considerably upon systematic acidification of the extra- and intracellular growth medium (Kennedy et al., 1985). Protonic acids (and therefore, physiologically inaccessible pH values) need not necessarily be invoked as the acid source in light of the recent finding that MC is efficiently activated by Lewis acidic metal complexes (Iyengar et al., 1986). The possibility furthermore exists that the initial explusion of methanol from MC via enzyme-assisted proton transfer may be responsible for the release of activated MC molecules into the surrounding milieu. Evaluation of the activation mechanism of MC in vivo can presumably now be made by analysis of the adducts obtained from DNA exposed to MC in vivo, as it is now clear that the adduct distribution patterns reflect the MC activation mechanism by which they were produced. The simple preparation of MC adducts presented here should make standard adducts readily available for such investigations in the future.

M–Guanines. As ^{1}H NMR is generally not suited to unambiguously furnish the alkylation position on substituted guanines due to lack of proton signals, we have developed the techniques of differential second-derivative FTIR (SEDIR) and UV (SEDUV) spectroscopy, which serve to "fingerprint" alkylated guanines via their characteristic absorption frequencies (Verdine & Nakanishi, 1985a). Both of these methods are well suited to microgram structural studies and, when used in combination, provide a means of independently confirming the results gained from each other. Second differentiation of FTIR and UV spectra provide a simple protocol

for resolution enhancement of inherently broad spectral lines and thus facilitate extraction of all of the information contained in an absorbance-mode spectrum, as exemplified in this work.

The crucial point of 1″,2″-vicinal stereochemistry in **5** and **6** was discerned by taking advantage of the unambiguous relation between mitosene 1,2 stereochemistry and the sign of the ~530-nm circular dichroic Cotton effect (Tomasz et al., 1983, 1984). Knowledge of the vicinal stereochemistry has facilitated model-building studies aimed at understanding the interaction of activated MC with double-stranded DNA (see below).

M–dG$_I$. As mentioned above, M–dG$_I$ displays a complex pattern of at least four interconverting peaks on HPLC. All individual fractions, however, had the same UV spectra, which indicated the presence of an *N*7-alkyl-FAPyr riboside moiety. We have extended the useful range of the reported UV maxima for ring-opened *N*7-alkylguanosines to include the region from 220 to 200 nm and in doing so have found a characteristic new UV maximum at 218 nm that is uniquely present in only imidazolium-cleaved *N*7-alkylguanosines. This finding adds another useful marker for judging the presence or absence of the *N*7-alkyl-FAPyr structural element in complex drug–DNA adducts.

The results of the above UV studies, in combination with the finding that perchloric acid hydrolysis of M–dG$_I$ yielded no free Gua, indicated that the Gua base initially modified in the Gua-alkylation reaction had undergone subsequent degradative modification. Since adducts **5** and **6** arise through a known *acid-catalyzed* deribosylation reaction, we undertook a study to define the alternate *basic* degradation pathway of *N*7-alkylguanosines and *N*7-alkyl-2′-deoxyguanosines. From a comparison of the characteristic ^{1}H NMR and FTIR absorptions of model *N*7-alkyl-FAPyr compounds with the spectral properties of M–dG$_I$, we were able to conclude that the M–dG$_I$ mixture consists of a series of ring-opened *N*7-mitosenyl-2′-deoxyguanosines, **7–9**, which differ in the nature of their sugar moieties. The complex behavior of M–dG$_I$ on HPLC can be understood on the basis of (i) the ability of **7–9** to interconvert chemically through a common N9/C-1′ imine intermediate (not shown) and (ii) the occurrence of rotameric isomers in each of the M–dG$_I$ components. In our hands, the latter rotamers were directly observed (by ^{1}H NMR) in all *N*7-alkyl-FAPyr compounds. Since all of the components of M–dG$_I$ interconvert, it follows that **7–9** all possess the same mitosene 1″ stereochemistry, as epimerization at the 1″-position is excluded under the mild conditions employed in the HPLC analysis. The mixture of **7–9** shows a positive circular dichroic CE at 550 nm, thus indicating that the FAPyr moiety is linked to the 1″β-position in all three isomers.

Relative Distribution of the Glycosidic Cleavage and FAPyr–MC Adducts (**5**/**6** *and* **7–9**). The relative amounts of M–guanine products **5**/**6** with respect to imidazolium-cleaved adducts **7–9** (Table I) varies with the reaction conditions in a manner that is in accord with the known principles of *N*7-alkylguanine nucleoside chemistry (Lawley & Brookes, 1963). That is (i) low pH promotes glycosidic bond cleavage and suppresses imidazolium cleavage, thus leading to the formation of *N*7-mitosenylguanine derivatives **5** and **6**, (ii) high pH favors imidazolium cleavage and thus leads to a predominance of the *N*7-mitosenyl-FAPyr adducts **7–9** and little, if any, of the *N*7-alkylguanines **5**/**6**, and (iii) both of the above processes are faster for *N*7-alkyl-2′-deoxyguanosines than the corresponding ribo series. Thus the ratio (**5** + **6**)/**7–9** is extremely low (nil) under the pH 7–8 conditions employed in the reductive activation of MC (Table I, entries A/D); under the current acidic conditions (pH 3.5–5), a much greater relative amount of the *N*7-mitosenylguanines **5** + **6** is observed, even when the sugar moiety is changed to ribose (Table I, entries B/C/E–G).

A notable difference does exist between the observed decomposition rates of model *N*7-ethylguanosine (**11**) and the putative *N*7-mitosenyl-dG intermediate **10**. Model **11** is stable at pH values between approximately 3.5 and 8.5 for several hours and in neutral lyophilized powders for several months at room temperature. Intermediate **10**, on the other hand, has never been observed directly in any reaction of MC regardless of the substrate or activation conditions; thus it appears that **10** is extremely unstable over the entire range of pH values, giving rise to products **5**/**6** and **7–9** in ratios depending on slight changes in the pH of the medium. This behavior is consistent with reports that *N*7-(2-aminoethyl)guanosine and -deoxyguanosine exhibit an unusually strong tendency to undergo imidazolium ring fission and depurination; for example, the half-life of *N*7-(2-aminoethyl)-2′-deoxyguanosine is only ~5 min at pH 7.7, 25 °C (Hemminki, 1984). Additionally, Mueller and Eisenbrand (1985) reported that *N*7-(2-aminoethyl)guanosine underwent imidazolium fission 100 times faster than the corresponding *N*7-ethyl compound **11**. Since **10** possesses the analogous *N*7β-aminoalkyl structural entity, its rapid degradation in aqueous solution at any pH value is fully anticipated.

It is notable, however, that *in DNA* the behavior of the *N*7-mitosenyl residue **10c** is different from that observed in the nucleoside and dinucleoside phosphate cases. As seen in Table I (entry H), at the pH values employed for the acidic activation of MC in the presence of DNA, none of the adducts **7–9** are observed (subsequent to enzymatic digestion procedures, including an SVD digest for several hours at pH 8.5). Evidently, the imidazolium opening pathway of **10** is strongly suppressed when such a structural element is incorporated into DNA. Decreased hydrolysis reaction rates upon going from the mononucleotide to the double-stranded polynucleotide is a commonly observed phenomenon, e.g., in the imidazolium hydrolysis of *N*7-methylguanine residues in DNA (Hendler et al., 1970). M–dG$_I$ (**7–9**) consists of a series of compounds all of which possess 1″β-stereochemistry (1″,2″-cis) and thus arise from the DNA-bound precursor 1″β-**10c**. As mentioned above, 1″β-**10c** appears to be exceedingly unstable to glycosidic bond cleavage, as evidenced by the spontaneous and quantitative release of M–guanine **6** from MC-modified DNA. The failure to observe any M–dG$_I$ adducts upon enzymatic digestion of the MC–DNA complex thus appears to result directly from the dramatic acceleration of the glycosidic bond cleavage of 1″β-**10c**; the imidazolium cleavage reaction of 1″β-**10c** is apparently no longer rate competitive. Simply stated, all of the 1″β-**10c** has undergone deribosylation of **6** before sufficient time has evolved for imidazolium fission of 1″β-**10c** to occur.

The glycosidic cleavage reaction of 1″α-**10c** is evidently retarded relative to that observed for 1″α-**10a** or 1″α-**10b**, since *N*7-mitosenylguanine **5** is released into the medium not only during the MC–DNA alkylation reaction (both **5** and **6** released) but also later during the enzymatic digestion of the MC–DNA reaction (only **5** released; Methods, Figure 3, and discussion above). Thus it appears that the lifetime of the putative initial adduct 1″α-**10** is somewhat longer in DNA than in the low molecular weight nucleoside and dinucleoside phosphate cases; a rigorous comparison of the relative lifetimes of 1″β-**10a**, -**10b**, and -**10c** will require further kinetic studies owing to the inherent complexity of their bidirectional deg-

radation pathway. It is, however, evident that the proximal 2″β-amino group has a profound influence on the relative rate of imidazolium ring fission of **10a/b**. Namely, when the 1″,2″ substituents in **10a/b** are oriented cis, the imidazolium ring fission is considerably faster than in the case of 1″,2″-trans stereochemistry; this phenomenon is presumably manifested as a result of internal base catalysis in which the 2″β-NH_2 group ($pK_a \sim 8.5$) deprotonates a water molecule in the immediate vicinity of the electrophilic imidazolium C-8, thus resulting in an accelerated hydrolysis reaction. Such an internal catalysis mechanism intrinsically requires that 2″β-amino group be on the same face of the mitosene carbon skeleton as exists only in the 1″β-isomer of **10a/b**. Presumably, the same internal base catalysis is responsible for the accelerated imidazolium hydrolysis of *N*7-(2-aminoethyl)-2′-deoxyguanosine, though considerations of the side-chain stereochemistry do not apply in that case.

Cross-Linking of DNA by Acid-Activated MC. Lown et al. (1976) observed that covalent cross-links are formed in DNA exposed to MC in vitro in an acidic medium similar to the conditions employed in this study. These conclusions were based on the reversible melting behavior of MC-treated DNA and are analogous to the well-known DNA cross-linking effect of reductively activated MC (Szybalski & Iyer, 1967). Very recently we isolated and chemically identified an MC–$(dG)_2$ adduct that is responsible for the DNA cross-linking manifestations of MC^{*H} (Tomasz et al., 1987). No evidence for the formation of the same bifunctional adduct was obtained, however, under the present acidic MC-activating conditions. Specifically, HPLC traces (not shown) of MC^{*+}-treated DNA show no peak corresponding to an authentic sample of the M–$(dG)_2$ adduct. Negative results were also obtained with poly(dG-dC)·poly(dG-dC) as substrate for MC^{*+} even though this polymer is an especially rich source of the MC^{*H}-induced cross-link (Tomasz et al., 1987). It thus appears that (i) the MC^{*+}-induced cross-links are different from those induced by MC^{*H} and/or (ii) they are formed in quantities below the level of UV detection, and/or (iii) MC–DNA cross-links are not actually formed under acidic activation.

Multiple Interconverting Components of the Imidazole Ring Fission Products of N7-Ethyl- and N7-Methylguanosine and N7-Methyl-2′-deoxyguanosine. The phenomenon of room temperature interconversion has previously been observed for the cleavage products of *N*7-methylguanosine (Chetsanga & Makaroff, 1982); however, in that study no explanation was offered for the observed behavior. We have determined that the inherent complexity of ring-opened *N*7-alkylguanosines is primarily due to the presence of three distinct *N*7-alkyl-FAPyr ribosides, which are identical except in their sugar moiety; furthermore, the three components are capable of interconverting chemically through a common N9/C-1′ imine intermediate (as in **12**, Scheme II) to regenerate the original mixture from any one pure component. Though most of the studies performed in the past on *N*7-alkylguanosines have focused on *N*7-methylguanosine **26**, we have found that *N*7-ethylguanosine (**11**) yields FAPyr derivatives **13–15**, which are more easily separable and are therefore better suited for structural studies.

Acetylation of **13–15** furnishes chemical derivatives **16–18**, which are readily isolable and directly furnish the requisite information concerning the nature of the attached ribose moiety. Analysis of the ^1H NMR chemical shifts for the 2′-, 3′-, 4′-, and 5′-proton signals allowed the assignment of furanose triacetate to **16** and **17** (also **13** and **14**, by chemical conversion) as well as that of pyranose triacetate to **18** (also **15**, by chemical conversion). As **16** and **17** possess a five-membered sugar ring, the usage of coupling constants was precluded (*J* values are too close in 1′/2′-cis and -trans); furthermore, the six-membered sugar of **18** gives rise to vicinal coupling–coupling constants that are indicative of a nonchair conformation, again precluding the usage of coupling constants (range of possible conformations to fit *J* values too large to assign unique configuration). Owing to the complexity of Karplus analysis of ^1H NMR spectra for **16–18**, we turned to NOE experiments to unambiguously solve the 1′ configurations of **16–18**. NOE experiments were initially attempted in Me_2SO-d_6 solvent; however, the large enhancements observed to the H_2O signal raised the possibility of observing spurrious NOE effects due to spin-diffusion processes. Successful NOE experiments were obtained upon changing the solvent to Me_2CO-d_6. On the basis of the above NOE experiments, we have assigned the full sugar moieties in **16–18** as follows: (**16**) 1′β-ribofuranoside 2′,3′,5′-triacetate; (**17**) 1′α-ribofuranoside 2′,3′,5′-triacetate; (**18**) 1′β-ribopyranoside-2′,3′,4′-triacetate. In no case was the corresponding 1′α-ribopyranoside epimer of **18** observed, presumably due to unfavorable steric interactions that render the product (i.e., 1′α-**15**) thermodynamically disfavored. Furthermore, imine **12** was not observed directly (even by ^1H NMR), probably because the reclosure reaction involving the 4′- or 5′-OH group (Scheme II) is extremely fast.

An analogous pathway for the alkali-catalyzed imidazole ring fission of the synthetic nucleoside 9-β-D-ribofuranosylpurine was recently reported by Lönnberg and Lehikoinen (1984). In that case, NMR evidence for the formation of all four possible riboside isomers was presented; however, the products were not rigorously characterized. It is clear from our experiments that even after long reaction times (>5 h) in 2 N NH_4OH only three products are predominantly formed in the hydrolysis mixtures of *N*7-alkylguanine ribosides **11**, **19**, and **26**.

For correlation with the 2′-deoxyribo series, we also performed the basic hydrolysis of *N*7-methyl-2′-deoxyguanosine (**19**) and found that it similarly gives rise to primarily three rearranged *N*7-methyl-FAPyr 2′-deoxyribosides. These three were similarly converted to the corresponding diacetates; upon HPLC it was possible to isolate isomer **25** in pure form and isomers **23/24** as a mixture. ^1H NMR measurements on **25** led to the assignment of 1′β-(*N*7-methyl-FAPyr)-2′-deoxyribopyranose 3′,4′-diacetate; similar analysis of the **23/24** mixture revealed that it consists of the 1′α- and 1′β-anomers of (*N*7-methyl-FAPyr)-2′-deoxyribofuranose 3′,5′-diacetate. It is quite possible that the latter two are inseparable owing to the fact that they chemically interconvert under HPLC conditions (interconversion with **25** is blocked by acetylation of its 4′-OH).

Nature of the N-Formyl Rotamers in N7-Alkyl-FAPyr Ribosides. On the basis of ^1H NMR data and chromatographic behavior, it is observed that each distinct riboside isomer exists in solution as four additional structural isomers related to each other by simple bond rotations (rotamers). Some evidence relevant to the precise nature of these rotamers has been reported by Boiteux et al. (1984), who examined the isomerism of the deribosylated *N*7-alkyl-FAPyr base **36**. In that study, it was indicated (on the basis of NOE experiments) that **36** exists as *two* rotamers, **36A** (minor rotamer) and **36B** (major rotamer), related to each other by 180° rotations about the C-5/N7 and N7/C-8 bonds. In contrast, by the arguments given below, we have determined that the four rotamers of **16** correspond to structures **16A–16D**. In an attempt to correlate

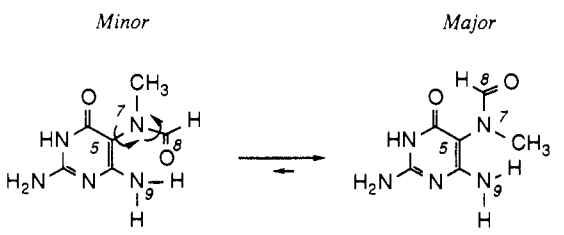

the results obtained on **36** with our observation of *four* rotamers in the case of ribose-bearing *N*7-FAPyr compounds, NOE experiments were performed on (*N*7-ethyl-FAPyr)-β-ribofuranose triacetate **16** with particular attention to the relative orientation of groups in the N9/C-8 area. In contrast to the findings observed for **36**, in no experiment was an NOE enhancement observed between N9-H and the protons of the *N*7-ethyl group; instead, upon irradiation of the high-intensity N9-H signals of **16** at 7.38 and 7.23 ppm (NOE experiment not shown; see Figure 14 for ^{1}H NMR of **16**), a reproducible ~5% NOE is transmitted to the 8-C*H*O of the major formyl rotamer at 7.71 ppm. Such an NOE is not possible in structure **16E**, and thus it appears that the rotamer corresponding to **36E** is not significantly populated in **16**. On the other hand, irradiation of the low-intensity N9-H signal at 6.94 ppm (Figure 14) gives rise to a weak NOE (~2%) in the 8-C*H*O signal of the minor formyl rotamer at 8.11 ppm. These data, taken together, suggest that the sets of major and minor formyl rotamers in **16** are related to each other by 180° rotation about the amide bond and are simply the result of amide syn/anti isomerism. Thus, the major set of rotamers are assigned as **16A/B** while the minor set of rotamers correspond to **16C/D**.

It is not immediately evident why *four* isomers are produced when a single 180° bond rotation should seemingly produce only *two* rotamers. The resolution of this issue becomes clear upon closer inspection of the structure of **16**. Examination of the array of atoms from N9-H to 8-CHO reveals that an unavoidable steric interaction exists if one constrains coplanarity upon all of the atoms in the array (coplanarity should maximize p–π orbital overlap). Thus, some of the atoms are forced from coplanarity in order to avoid energetically unfavorable interactions; as a result, the N9–C-8 atomic arrangement takes on a screw sense, which can either be positive or negative (structures **16A–16D**). Given this scenario, the N9–C-8 system behaves as a chiral center. If no other chiral centers are present as in **36**, the FAPyr screw-related isomers are enantiomeric and thus are not observed by NMR. On the other hand, if the molecule bears one or more additional chiral centers (as in **16**), the screw sense of the FAPyr array gives rise to two *diastereomers* for each formyl rotamer (i.e., **16A/B** and **16C/D** are diastereomeric). Thus, since rotation of the *N*-formyl group is slow on the NMR time scale (Boiteux et al., 1984), all four possible rotamers are diastereomeric and therefore observed directly.

These findings represent an important addition to the chemistry of the imidazole ring fission of *N*7-alkylguanosines. In the original papers that report the discovery of the ring opening of *N*7-methylguanosine (Brookes & Lawley, 1961; Haines et al., 1962; Townsend & Robins, 1963) a single structure was assigned to the product (i.e., **16**, Et = Me) and this was extended by analogy to the *N*7-ethylguanosine ring-opened product (Brookes & Lawley, 1963; Singer, 1972). The failure to demonstrate a mixture of compounds in both of these cases is quite understandable in light of the facts that (i) reversed-phase HPLC, relied upon heavily in this study, was not available at the time of the earlier studies; (ii) the mixtures generated from ring opening of all compounds used in this study gave a single spot on paper chromatography, as reported in the original literature, and (iii) high-resolution NMR and modern NMR methods, including NOE experiments, were not practically available until quite recently. Anomerization of **16** and related compounds, however, is not unexpected since primary and secondary glycosylamines are known to anomerize rapidly via an acyclic schiff base (as in **12**) in a base-catalyzed process [for review, see Capon (1969)]. While this phenomenon has been demonstrated rigorously in the cases of ring-opened **11**, **19**, and **26**, it is reasonable to assume that the same anomerization process is operative in the formation of **7–9** from **10**. The presence of multiple HPLC and ^{1}H NMR peaks for the M–dG$_I$ mixture further strengthens this assertion. We thus propose that the anomerization of *N*7-alkyl-FAPyr ribosides is a general phenomenon and that only three of the four possible ribose isomers are significantly populated in this reaction under equilibrating conditions. It is probable that the nature of the attached *N*7-alkyl group and the N9 sugar moiety has a strong modulating influence on the rate of imidazolium opening as well as the observed product distribution of rearranged ribosides. A systematic study of these factors is warranted by the findings reported here.

Although the formation of the various *N*7-Gua–MC adducts reported here remains to be demonstrated in vivo, the new multiple-structure adducts of the imidazolium-cleaved alkylated guanosines have more general implications. Many biologically important DNA-modifying agents including dimethylnitrosamine (Beranek et al., 1983), phosphoramide mustard (Chetsanga et al., 1982), and aflatoxin B$_1$ (Hertzog et al., 1980; Croy & Wogan, 1981) are known to induce the formation of *N*7-alkyl-FAPyr sites in vivo. Interestingly, these sites exist in cellular DNA as "persistent lesions"; i.e., they are slow to be repaired in vivo (above references). They also function as replication blocks in vitro (Boiteux & Laval, 1983; Refolo et al., 1985). Furthermore, Lagravere et al. (1984) have shown the *N*7-alkyl-FAPyr residues in DNA are not corrected by a FAPyr-specific DNA glycosylase enzyme in vitro when the modified DNA is present in the Z form. In light of the present work, the potential exists that such *N*7-alkyl-FAPyr sites, once formed, could undergo epimerization to the 1′α-deoxyribose form at the DNA level. This in turn could have a profound effect on enzymatic repair, replication, DNA secondary structure, and other functional properties of cellular DNA. Some of these issues are currently under investigation in our laboratories.

ACKNOWLEDGMENTS

We thank Dr. W. T. Bradner of Bristol Laboratories, Syracuse, NY, for a generous supply of mitomycin C and Harriet Stratis for experimental assistance in the early stages of this research program.

REFERENCES

Bean, M., & Kohn, H. (1983) *J. Org. Chem. 48*, 5033–5041.
Beranek, D. T., Weis, C. C., Evans, F. E., Chetsanga, C. J., & Kadlubar, F. F. (1983) *Biochem. Biophys. Res. Commun. 110*, 625–631.
Boiteul, S., & Laval, J. (1983) *Biochem. Biophys. Res. Commun. 110*, 552–558.
Boiteux, S., Belleney, J., Roques, B. P., & Laval, J. (1984) *Nucleic Acids Res. 12*, 5429–5439.
Brookes, P., & Lawley, P. D. (1961) *J. Chem. Soc.*, 3923–3928.
Capon, B. (1969) *Chem. Rev. 69*, 407–498.

Chetsanga, C. J., & Makaroff, C. (1982) *Chem.-Biol. Interact. 41*, 235–249.
Chetsanga, C. J., Polidori, G., & Mainwaring, M. (1982) *Cancer Res. 42*, 2616–2621.
Croy, R. G., & Wogan, G. N. (1981) *Cancer Res. 41*, 197–203.
Croy, R. G., Essigmann, J. M., Reinhold, V. N., & Wogan, G. N. (1978) *Proc. Natl. Acad. Sci. U.S.A. 75*, 1745–1749.
Douglass, H. O., Lavin, P. T., Goudsmit, A., Klassen, D. J., & Paul, A. R. (1984) *J. Clin. Oncol. 2*, 1372–1377.
Farmer, P. B., Foster, A. B., Jarman, M., & Tisdale, M. J. (1973) *Biochem. J. 135*, 203–213.
Haines, J. A., Reese, C. B., & Lord Todd (1962) *J. Chem. Soc.*, 5281–5288.
Hashimoto, Y., Shudo, K., & Okamoto, T. (1982) *Tetrahedron Lett.*, 677–680.
Hashimoto, Y., Shudo, K., & Okamoto, T. (1983) *Chem. Pharm. Bull. 31*, 861–869.
Hashimoto, Y., Shudo, K., & Okamoto, T. (1984) *Acc. Chem. Res. 11*, 403–408.
Hemminki, K. (1984) *Chem.-Biol. Interact. 48*, 249–260.
Hendler, S., Fürer, E., & Srinivasan, P. R. (1970) *Biochemistry 9*, 4141–4153.
Hertzog, P. J., Lindsay-Smith, J. R., & Garner, R. C. (1980) *Carcinogenesis 1*, 787.
Hornemann, U., Iguchi, K., Keller, P. J., Vu, H. M., Kozlowski, J. F., & Kohn, H. (1983) *J. Org. Chem. 48*, 5026–5033.
Iyengar, B. S., Takahashi, T., Remers, W. A., & Bradner, W. T. (1986) *J. Med. Chem. 29*, 144–147.
Iyer, V. N., & Szybalski, W. (1964) *Science (Washington, D.C.) 145*, 55–58.
Kasai, H., Nakanishi, K., & Traiman, S. (1978) *J. Chem. Soc., Chem. Commun.*, 798–800.
Kennedy, K. A., Sligar, S. G., Polomski, L., & Sartorelli, A. C. (1982) *Biochem. Pharmacol. 31*, 2011–2016.
Kennedy, K. A., McGurl, J. D., Leondaridis, L., & Alabaster, O. (1985) *Cancer Res. 45*, 3541–3547.
Keyes, S. R., Fracasso, P. M., Heimbrook, D. C., Rockwell, S., Sligar, S. G., & Sartorelli, A. C. (1984) *Cancer Res. 44*, 5638–5643.
Kohn, H., & Zein, N. (1983) *J. Am. Chem. Soc. 105*, 4105–4106.
Lagravère, C., Malfoy, B., Leng, M., & Laval, J. (1984) *Nature (London) 310*, 798–800.
Lawley, P. D., & Brookes, P. (1963) *Biochem. J. 89*, 127–138.
Lee, D. C., Hayward, J. A., Restall, C. J., & Chapman, D. (1985) *Biochemistry 24*, 4364–4373.
Lin, A. J., Cosby, L. A., & Sartorelli, A. C. (1976) *ACS Symp. Ser. No. 30*, 71–80.
Lönnberg, M., & Lehikoinen, P. (1984) *J. Org. Chem. 49*, 4964–4969.
Lown, J. W., & Weir, G. (1978) *Can. J. Biochem. 56*, 296–304.
Lown, J. W., Begleiter, A., Johnson, D., & Morgan, A. R. (1976) *Can. J. Biochem. 54*, 110–119.
McClelland, R. A., & Lam, K. (1985) *J. Am. Chem. Soc. 107*, 5182–5186.
Moore, H. W. (1977) *Science (Washington, D.C.) 197*, 527–532.
Mueller, N., & Eisenbrand, G. (1985) *Chem.-Biol. Interact. 53*, 173–181.
Pan, S.-S., Andrews, P. A., Glover, C. J., & Bachur, N. R. (1984) *J. Biol. Chem. 259*, 959–966.
Pullman, A., & Pullman, B. (1981) *Q. Rev. Biophys. 14*, 289–380.
Refolo, L. M., Conley, M. P., Sambamurti, K., Jacobsen, J. S., & Humayun, M. Z. (1985) *Proc. Natl. Acad. Sci. U.S.A. 82*, 3096–3100.
Schwartz, H. S., Sodergren, J. E., & Philips, F. S. (1963) *Science (Washington, D.C.) 142*, 1181–1183.
Shirahata, N., & Hirayama, K. (1983) *J. Am. Chem. Soc. 105*, 7199–7200.
Singer, B. (1972) *Biochemistry 11*, 3939–3947.
Singer, B., & Grunberger, D. (1983) *Molecular Biology of Mutagens and Carcinogens*, Plenum, New York.
Susi, H., & Byler, D. M. (1983) *Biochem. Biophys. Res. Commun. 115*, 391–397.
Szybalski, W., & Iyer, V. N. (1967) in *Antibiotics I: Mechanisms of Action* (Gottleib, D., & Shaw, P. D., Eds.) p 230, Springer-Verlag, New York.
Taylor, W. G., & Remers, W. A. (1975) *J. Med. Chem. 18*, 307–311.
Tomasz, M., & Lipman, R. (1979) *J. Am. Chem. Soc. 101*, 6063–6067.
Tomasz, M., & Lipman, R. (1981) *Biochemistry 20*, 5056–5061.
Tomasz, M., Mercado, C. M., Olson, J., & Chatterjie, N. (1974) *Biochemistry 13*, 4878–4887.
Tomasz, M., Lipman, R., Snyder, J. K., & Nakanishi, K. (1983) *J. Am. Chem. Soc. 105*, 2059–2063.
Tomasz, M., Jung, M., Verdine, G. L., & Nakanishi, K. (1984) *J. Am. Chem. Soc. 106*, 7367–7370.
Tomasz, M., Lipman, R., Verdine, G. L., & Nakanishi, K. (1985) *J. Am. Chem. Soc. 107*, 6120–6121.
Tomasz, M., Lipman, R., Verdine, G. L., & Nakanishi, K. (1986a) *Biochemistry 25*, 4337–4344.
Tomasz, M., Dondapati, C., Lipman, R., Shimotakahara, S., Veiro, D., Walker, V., & Verdine, G. L. (1986b) *Proc. Natl. Acad. Sci. U.S.A. 83*, 6702–6706.
Tomasz, M., Lipman, R., Dondapati, C., Pawlak, J., Verdine, G. L., & Nakanishi, K. (1987) *Science (Washington, D.C.)* (in press).
Verdine, G. L., & Nakanishi, K. (1985a) *J. Am. Chem. Soc. 107*, 6118–6120.
Verdine, G. L., & Nakanishi, K. (1985b) *J. Chem. Soc., Chem. Commun.*, 1093–1095.
Webb, J. S., Cosulich, D. B., Mowat, J. H., Patrick, J. B., Broschard, R. W., Meyer, W. E., Williams, R. P., Wolf, C. F., Fulmor, W., Pidacks, C., & Lancaster, J. E. (1962) *J. Am. Chem. Soc. 84*, 3185–3187.